Preparation and Application of starch nanoparticles for nanocomposites: A review

ARTICLE *in* REACTIVE AND FUNCTIONAL POLYMERS · OCTOBER 2014

Impact Factor: 2.52 · DOI: 10.1016/j.reactfunctpolym.2014.09.020

2 AUTHORS:

Deborah Le Corre
Plant and Food Research
25 PUBLICATIONS **399** CITATIONS
SEE PROFILE

Hélène Angellier-Coussy
Université de Montpellier
40 PUBLICATIONS **1,122** CITATIONS
SEE PROFILE

Reactive & Functional Polymers 85 (2014) 97–120

Contents lists available at ScienceDirect

Reactive & Functional Polymers

journal homepage: www.elsevier.com/locate/react

Review

Preparation and application of starch nanoparticles for nanocomposites: A review

Déborah Le Corre [a,*], Hélène Angellier-Coussy [b]

[a] Plant & Food Research Ltd., Private Bag 4704, Christchurch Mail Centre, Christchurch 8140, New Zealand
[b] Unité Mixte de Recherche «Ingénierie des Agropolymères et Technologies Emergentes», INRA/ENSA.M/UMII/CIRAD, Université Montpellier II, CC023, pl. E Bataillon, 34095 Montpellier Cedex, France

ARTICLE INFO

Article history:
Received 11 June 2014
Received in revised form 17 July 2014
Accepted 23 September 2014
Available online 28 October 2014

Keywords:
Starch
Nanoparticles
Reactive
Nano-fillers
Nano-composites

ABSTRACT

The increasing scientific and industrial interest for starch nanoparticles (SNP) has led to the development of numerous methods for preparing sub-micron starch fillers for nanocomposites applications. Starch nanocrystals (SNC), which constitute the focus of this review, are one type of SNP with crystalline property and platelet like morphology. SNC can be extracted from various starch botanical sources, allowing to obtain a large range of amylose content, shape, viscosity in suspension, surface reactivity and thermal resistance. To date, the most common method for extracting SNC remains the mild acid hydrolysis of the amorphous parts of native granular starch. So far, alternative methods render much lower yield. Since first publications on SNC, the principal aim is to use them as reinforcement in polymer matrices. Thanks to the reactive nature of starch, SNC surface can be modified by grafting or cross-linking which renders them more readily dispersible in the polymer matrix. The present review focus on the reinforcing effect and mechanisms of SNC, as well as on their impact of barrier properties of polymers.

Contents

* Corresponding author.
E-mail address: Deborah.lecorre@plantandfood.co.nz (D. Le Corre).

http://dx.doi.org/10.1016/j.reactfunctpolym.2014.09.020
1381-5148/

1. Introduction

Starch is a renewable and biodegradable polymer produced by many plants as a source of storage energy. Humans and their ancestors have always used starchy products. Starch grains have recently (2010) been identified from grinding stones in Europe (Italy, Czech Republic and Russia) dating back to 30,000 years ago [1]. The practical use of starch products (i.e. non-food application) developed when Egyptians cemented strips of papyrus together with starch adhesive made from wheat [2]. Later (from 700 AD) rice starch was used as surface treatment of Chinese papers. Romans also used it in cosmetic creams, to powder the hair and to thicken sauces [3]. Nowadays, main uses of starch have not changed much, with around 60% being used for food and 40% for industrial applications (as described in Fig. 1.16) [4]. Carbohydrate chemists have developed numerous products that have greatly expanded starch use and utility. In 2010, the world starch market was estimated to be 68 million tons [5]. The value of the output is worth □48.8 billion per year, explaining the industrialists and researchers seeking for new properties or high value application.

Most starches in the native form present limitations such as high viscosity, susceptibility to retrogradation, limited digestibility for some, and limited solubility for others. For this reason, most starch used in Food or Industrial applications is first modified [6]. Starches are chemically and/or physically modified to accentuate their positive characteristics, diminish their undesirable qualities (such as high viscosity, susceptibility to retrogradation, and lack of process tolerance), or add new attributes (retention, film formation, digestibility, solubility, etc.). Indeed, mild acid hydrolysis has been used for a long time to modify starch and its properties. In industry, starch slurries are treated with dilute HCl or H_2SO_4 at 25–55 °C for various periods of time, to produce "acid-modified" starch used as sizing agents, in gum candies production, and in paper and paper board production. Recent publications use either of these two acids for preparing starch nanocrystals.

Adding to its renewable nature, relatively low cost and world wide availability, starch is also perceived as an attractive filler to replace fossil-based ones such as carbon black in nanocomposites applications. Carbon black is manufactured by burning oil or natural gas in controlled conditions. It is the most important reinforcing agent used in the rubber industry. In fact, because of its origin from petroleum, carbon black causes pollution and gives to the rubber a black colour. Starch nanoparticles on the contrary are fully renewable and reactive nanoparticles, which have shown good reinforcing and barrier properties associated with white or transparent colours. This explains the increasing number of journal papers recently published on starch nanocrystals as shown in Fig. 1.

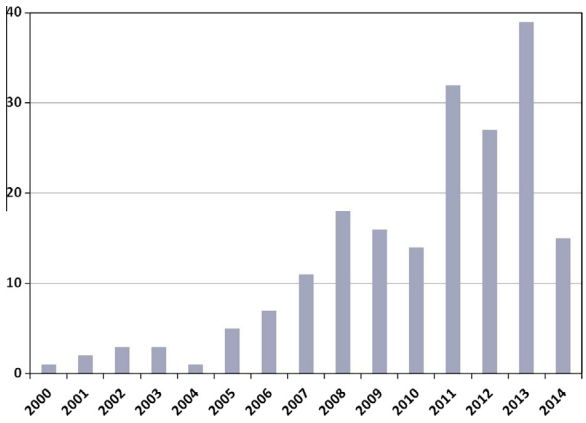

Fig. 1. Evolution of the number of journal articles and patents published with key word "starch nanocrystals". From SciFinder 20/05/2014.

This paper aims at reviewing the different types of starch nano-reinforcements, including starch nanoparticles (SNP) and more particularly starch nanocrystals (SNC), with a focus on their intrinsic properties, possible modification and application to the field of nanocomposites.

2. Starch nano-reinforcements types

2.1. Starch structure

The predominant model for starch structure is multi-scale and consists in the (a) granule (2–100 μm), into which we find (b) growth rings (120–500 nm) composed of (d) blocklets (20–50 nm) made of (c) amorphous and crystalline lamellae (9 nm) [7] containing (g) amylopectin and (h) amylose chains (0.1–1 nm), as presented in Fig. 2.

Starch granules consist mainly of two glucosidic macromolecules named amylose and amylopectin. Amylose is a linear molecule of glucose units linked by (1–4) α-D-glycoside bonds, slightly branched by (1–6) α-linkages. Amylopectin is a highly branched polymer consisting of relatively short branches of α-D-(1–4) glycopyranose that are interlinked by α-D-(1–6)-glycosidic linkages approximately every 22 glucose units [8].

Starch granules consist of concentric alternating amorphous and semi-crystalline growth rings that grow by apposition from the hilum of the granule. Schematically, the semi-crystalline growth rings consist of a stack of repeated crystalline and

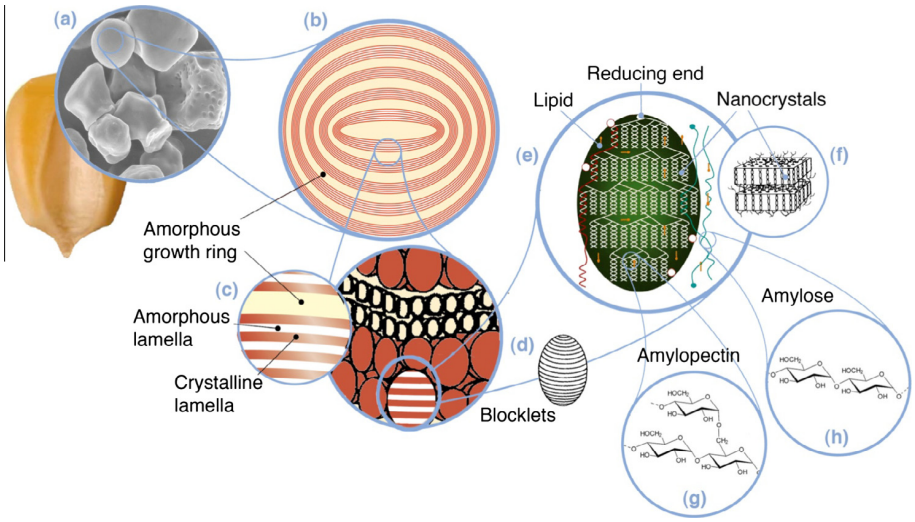

Fig. 2. Starch multi-scale structure. From [15] – Copyrights 2010 American Chemical Society. (a) Starch granules from normal maize (30 μm), (b) amorphous and semi-crystalline growth rings (120–500 nm), (c) amorphous and crystalline lamellae (9 nm): magnified details of the semi crystalline growth ring, (d) blocklets (20–50 nm): constituting unit of the growth rings, (e) amylopectin double helices forming the crystalline lamellae of the blocklets, (f) nanocrystals: other representation of the crystalline lamellae called SNC when separated by acid hydrolysis, (g) amylopectin's molecular structure, (h) amylose's molecular structure (0.1–1 nm). Reproduced with permissions from Gallant et al. [7] – Copyright 1997 Elsevier; Donald et al. [116] – Copyright Science and Technology Facilities Council 1997; and Tang et al. [117] – Copyright 2006 Elsevier.

amorphous lamellae (Fig. 2). The thickness of the combined layers is 9 nm regardless the botanic origin. It is believed that the crystalline region is created by the intertwining of chains with a linear length above 10 glucose units to form double helices [9] which are packed and form the crystallites; and the amorphous region corresponds to branching points. The number and thickness of these layers depend on the botanical origin of starch. They are thought to be 120–400 nm thick. Details on the structure of amorphous growth ring were not found in literature.

Until now, the location and state of amylose within granules is one of the most important questions remaining to be answered. Depending on the botanic origin of starch, amylose has been found in the amorphous region [10] (e.g. wheat starch), in bundles between amylopectin clusters [10], or interspersed among amylopectin clusters in both the amorphous and crystalline regions (e.g. normal maize starch) [10]. However, it has been demonstrated via cross-linking experiments using corn starch, that amylose molecules do not crosslink to one another, but do crosslink to amylopectin chains [11,12]. Thus, it invalidates the hypothesis of amylose chains forming bundles. The currently accepted model of amylose location in starch granule is therefore, as individual, radially-oriented chains randomly distributed among amylopectin chains [13]. Also, there is, now, evidence of an enrichment of amylose towards the periphery of the granule and that amylose molecules found towards the surface of the granules have shorter chain length than those located in the center [14].

2.2. Starch nanocrystals (SNC)

Starch nanocrystals (SNC) are crystalline platelets resulting from the disruption of the semi-crystalline structure of starch granules by the acid hydrolysis of amorphous parts, as presented in Fig. 2 [15].

First TEM observations (Fig. 3) by Putaux et al. [16] revealed the morphology of waxy maize starch nanocrystals produced after 6 weeks of hydrolysis. It showed: (a) a longitudinal view of lamellar fragments consisting of stack of elongated elements, with a width of 5–7 nm and (b) a planar view of individualized platelet after hydrolysis. Shapes and lateral dimensions were derived from observation of individual platelets in planar view: a marked

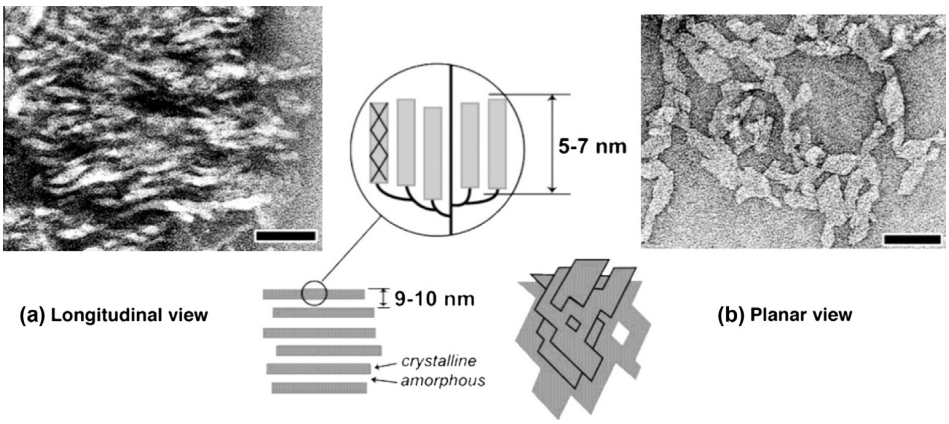

Fig. 3. First TEM observations of SNC: (a) longitudinal view and (b) planar view. Reproduced with permission from Putaux et al. [16] Copyright 2003 American Chemical Society.

60–65° acute angles for parallelepipedal blocks with a length of 20–40 nm and a width of 15–30 nm.

However, more recent publications report bigger SNC (40–70 nm for potato SNC [17]; 30–80 nm [18] and 60–150 nm [19,20] for pea SNC; and 50 nm [21] and 70–100 nm [22] for waxy SNC), with round edges [23] and found as grape-like aggregates of 1–5 μm. The heterogeneity in particle size could be explained by the differences in starch types but also by the difficulty to obtain well defined pictures of non-aggregated nanocrystals.

To the best of our knowledge, there are no commercial SNC currently available on the market. In fact, most patents dealing with SNC described either the modification of SNC [24–28] or their use in nanocomposites [29], and other applications [30]. The large majority of these patents are written and patented in Chinese. Very few describe a preparation method [31,32].

Starch crystallites, starch nanocrystals, microcrystalline starch and hydrolyzed starches all refer to the crystalline part of starch obtained by hydrolysis. They differ from each other in the extent of hydrolysis they have undergone (from the most to the least). They have to be distinguished from starch nanoparticles, of which they are just one kind, and which can be amorphous.

2.3. Starch nanoparticles (SNP) and commercial products

The aim of producing such nanocrystals or nanoparticles is to use them as fillers in polymeric matrices to improve their mechanical and/or barrier properties. Thus new and potentially more efficient processes have been tried out to produce starch nanoparticles by (i) precipitation of amorphous starch [33,34]; by (ii) combining complex formation and enzymatic hydrolysis [35] yielding in V-type nanocrystals (i.e. complexed with lipids) and by (iii) microfluidization [36]. Because these processes are very different, ensuing nanoparticles have different properties, crystallinity and shape. The processes for producing starch nanoparticles described in this section do not allow producing nanocrystals.

Ma et al. [33] prepared starch nanoparticles by precipitating dropwise gelatinised starch solution in ethanol. The suspension was centrifuged with ethanol to remove water and the settled material was dried at 50 °C to remove ethanol. The collected nanoparticles were used to prepare a bio-nanocomposite. Building on this, Ip et al. [37] most recently reported the possible co-precipitation of DNA with starch in the presence of ethanol, despite non existing charge attraction or specific binding mechanism. Hebeish et al. [38] proposed a modified solvent displacement method which integrates the use of a hydrophilic non ionic surfactant (polysorbate 80). Using 10% and 20% of this surfactant allowed preparing starch nanoparticles with smaller sizes (of respectively 112 nm and 102 nm) than those without surfactant (164 nm using dynamic light scattering).

Lim and Kim [39,40] filled two Korean patents on starch nanaoparticles formation. The first one claims starch /alcohol complex nanoparticles as in article from Kim and Lim [35] and the second, enzymatically hydrolyzed nanoparticles as reported in article from Kim et al. [41] and both represented in Fig. 4.

Liu et al. [36] transferred the method for producing microfibrillated cellulose (MFC) to the production of starch colloids. A 5% slurry of high amylose corn starch was ran through a Microfluidizer for several passes to obtain a gel-like suspension of nanometric particles which remained stable for more than a month. The resultant starch colloids were obtained from breaking down both amorphous and crystalline domains rendering an amorphous diffraction pattern after 10 passes.

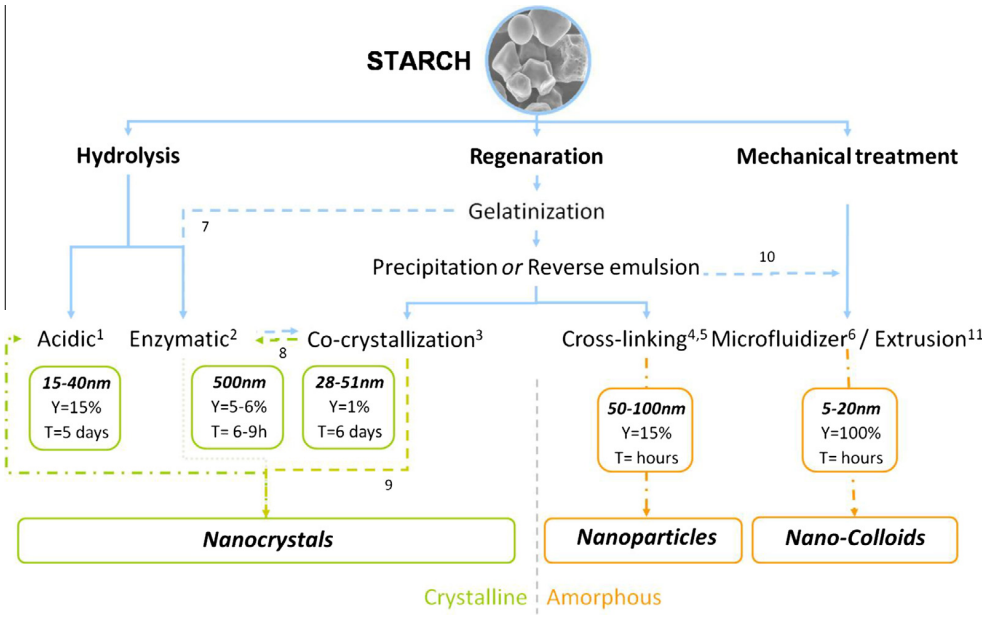

Fig. 4. Different ways of producing crystalline and amorphous starch nanoparticles, hydrolysis leads to nanocrystals, whereas regeneration and mechanical treatment lead to both amorphous and crystalline particles in final batch. Adapted from [15] – Copyrights 2010 American Chemical Society. (1) References to SNC production by acid hydrolysis as discussed in Section 3.1.1. (2) Temptative to produce SNC by enzymatic hydrolysis as reported by Kim et al. [64]. It is believe that the process leads to blocklets rather than nanoparticles. (3) Kim and Lim [35] report the preparation of nanocrystals by complex formation and (3) between amylose and n-butanol. They use enzymatic hydrolysis (8) to selectively keep crystalline particles. Classic path is (9). (4) Tan et al. [34] and (5) Ma et al. [33] report the production of starch nanoparticles by precipitation of gelatinized starch in non solvent followed by cross-linking reaction. (6) By analogy with microfibrillated cellulose (MFC), Liu et al. [36] intended producing starch nanoparticles by fluidization. It leads to crystalline microparticles turning into amorphous nanoparticles with an increasing number of runs. (7) and (8) Sun et al. [70] proposed combined enzymolysis followed by crystallisation. This is the inverse of the approach by Kim and Lim [35] whom first crystalised and then enzymatically hydrolyzed. (10) Shi et al. [118] propose a method for preparing submicron starch particles using a emulsion cross-linking technology using a high pressure homogenizer. In a following study [119] they report its spray-drying. (11) Not only homogenization (a.k.a. microfluidizer) can be used to mechanically modify the starch. A few studies including that of Song et al. [120] report the use of extrusion. Photos reproduced with permission from: Refs. [35,85,86] – Copyright (2003, 2008, 2009) American Chemical Society; Ref. [69] – Copyright 2009 Wiley-VCH Verlag GmbH & Co. KGaA; Ref. [87] – Copyright 2008 Elsevier; Ref. [88] – Copyright 2009 Elsevier.

Most popular starch nanoparticles commercial products are Eco-Sphere™ from Ecosynthetix and one grade of Mater-Bi™ from Novamont . They both fit the "Regenerated starch" nanoparticles category presented Fig. 3.

Eco-sphere™ by EcoSynthetix is a starch-based bio-latex substituting for oil-based latexes providing adhesive applications such as paper coating, tissue complexing or even as a replacement of polyvinyl acetate. The product is commercialized dry and has to be redispersed to form the latex [42]. WO Patent "Process for producing biopolymer nanoparticles" [43] written in English describes the reactive extrusion process used by EcoSynthetix.

Mater-Bi™ (Novamont) is a complexed destructurized and modified starch mixed with at least one hydrophobic polymer incompatible with starch such as Ecoflex™ (BASF) [44–46]. It is commercialized as pellets. Most famous application for Mater-Bi™ as a filler is BioTRED™, a bio-tire, developed in collaboration with Goodyear. Mater Bi™ was used to replace part of the lampblack and silica usually contained in the tire mixture [46].

Two other patents dealing with starch nanoparticles have been identified and relate to the production of starch nanoparticles for water treatment [47] and medical application [48].

3. Preparation of Starch nanocrystals

3.1. Hydrolysis

3.1.1. Acid Hydrolysis using chloridric or sulphuric acid

Although SNC are increasingly being investigated for different applications, there are only a limited number of articles studying their preparation and its influence on morphology (Table 1). Most studies report the production of starch nanocrystals from different starch sources using acid. Almost all of them refer to either of these two processes:

- Dufresne et al.'s process using HCl as previously discussed [49].
- Angellier et al.'s optimized process using H_2SO_4 [50]. In the later, "a given amount of starch granules (14.69 wt%/acid) is mixed with a given volume of 3.16 M H_2O_2 in an Erlenmeyer and stirred constantly at 100 rpm while maintained at 40 °C. After 5 days, the suspension is washed by successive centrifugations with distilled water until neutrality using centrifuge SIGMA 6K15, for 10 min at 10,000 rpm. The suspension is then submitted to a mechanical treatment with homogenizer Ultra Turrax for 2 min at 13,000 rpm to disperse aggregates and obtain a "stable" suspension. To avoid bacterial development during storage a few drops of chloroform are added to the suspension that is kept in a 4 °C cell."

Fig. 4 reports the hydrolysis kinetics for different starches and from different research groups.

For all starches a two-stage hydrolysis kinetics is evidenced, viz. (i) an initial fast hydrolysis step-presumably due to the hydrolysis of the amorphous regions of starch granules – and (ii) a second slower step presumably due to the hydrolysis of the more densely packed crystalline regions which do not allow readily the penetration of H_3O^+ [51,52]. Another hypothesis for the slower rate of hydrolysis in crystalline regions is that the hydrolysis of the glucosidic bonds requires a change in conformation from chair to half-chair [53]. Recently, Wei et al. [54] investigated the effect of defatting on the acid hydrolysis rate of maize starch with different amylase content. As can be seen in Fig. 5, defatting causes higher susceptibility of maize starch to acid hydrolysis. Compared to non-defatted waxy maize starch, the hydrolysis rate of defatted waxy maize starch is increased by 6% after 10 days.

The influence of acid and starch type on hydrolysis kinetic has been studied extensively by Singh and Ali [55–58]. Angellier et al. [50] also obtained a lower yield of hydrolysis with H_2SO_4 compared to HCl for the production of nanocrystals but showed that final suspensions were more stable with H_2SO_4 due to the postulated presence of sulphate groups at the surface (Fig. 6).

Following, Le Corre et al. [59] (DOE) measure the sulphate content of SNC prepared using sulphuric acid obtained after 1 μm filtration (F2). Results showed that measured sulphate content was much higher than that reported by Angellier [60] for a 3 M sulphuric acid hydrolyzed suspension (0.03%), and corresponded rather to values reported for non-filtered cellulose nanocrystals (CNC) (0.3–0.7%) [60]. Thus filtered individualized SNC should be even less susceptible to aggregation. Indeed, the suspension filtered at

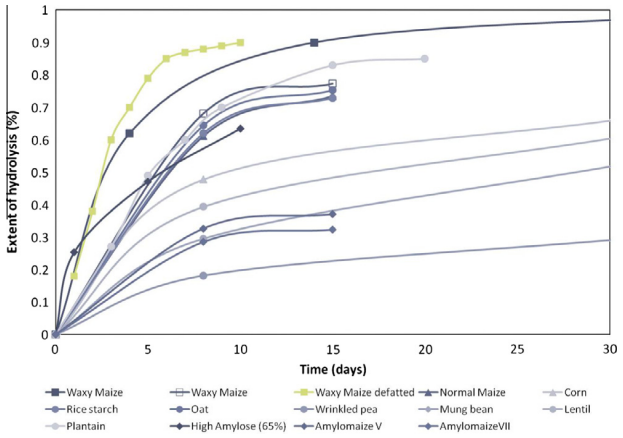

Fig. 5. Hydrolysis kinetic of different starches. High amylose (65%) from Li et al. [121]; waxy maize (■) from Angellier [122]; waxy maize, normal maize, amylomaize V, amylomaize VII, oat and rice starch from Jayakody et al. [51]; wrinkled pea, mung bean, lentil and corn from Robin et al. [123]; plantain from [124]; defatted waxy maize starch from [54].

Table 1
Preparation conditions of SNC and their characterization – adapted from original paper [15] for update. Copyrights 2010 American Chemical Society.

Botanic origin	Referred to as	Granular size (μm)	Amylose (%)[#]	Crystalline type	SNC diameter		SNC thickness	
					(nm)	Counts	(nm)	Counts
High amylose maize	**M70**	5–20	**65–75**	B	118 ± 53	190	5 ± 1.6[*]	76
Normal maize	**M27**	5–20	**27**	A	58 ± 36	576	8.3 ± 3.1[*]	112
Waxy maize	**M1**	5–20	**1**	A	47 ± 42	71	6.1 ± 1.9[**]	14
Wheat	**W28**	2–30	**28**	A	100 ± 50	71	3.7 ± 0.6[***]	30
Potato	**P21**	5–80	**21**	B	52 ± 4	951	7.6 ± 1.6[*]	31

[#] Supplier's data.
[*] Personnel measurements using software Gwyddon for image analysis.
[**] Conducted at «Service des Matériaux Polymères et Composites» (SMPC), Mons, Belgium.
[***] Personnel measurements on AFM software.

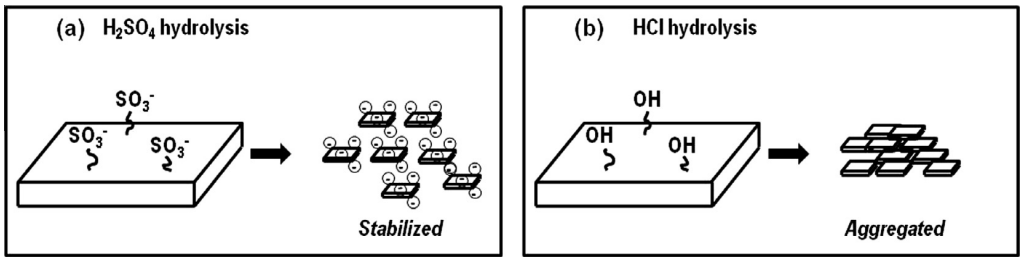

Fig. 6. Comparison between SNC prepared with (a) H_2SO_4 and (b) HCl.

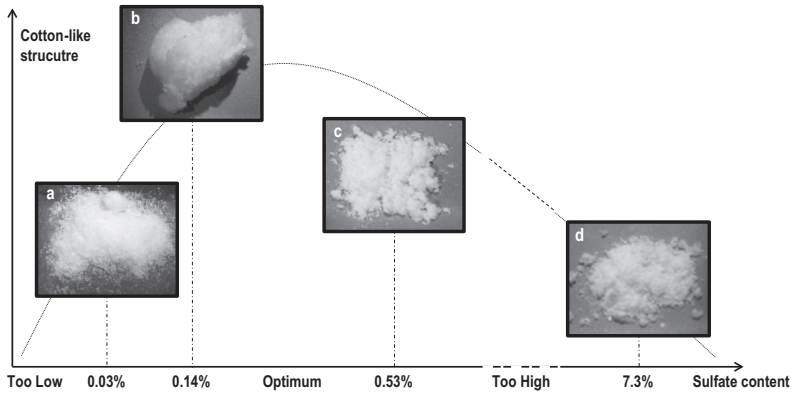

Fig. 7. Photographs of freeze-dried suspensions of F2 SNC with increasing sulphate content: (a) classic 5-days acid hydrolysis with 3.16 M H_2SO_4 with sulphate content 0.03% [60], (b) 4.5 M H_2SO_4 at 40 °C for 15 h, (c) 4.5 M H_2SO_4 at 25 °C for 15 h and (d) 3.75 M H_2SO_4 at 32.5 °C for 8 h. Reproduced with permission from [59].

1 μm (F2) has a cotton-like appearance after freeze-drying which suggests that particles are homogeneously smaller and better individualized than for particles filtered at 40 μm (F1). It was also found that there is an "optimal" acid concentration for which SNC presented enough surface sulphate groups to prevent aggregation, but not so much that they were degraded (dextrin) (Fig. 7).

Most recently, Wei et al. [61] studied the change in surface chemical composition of SNC after H_2SO_4 and HCl hydrolysis to explain the mechanism for better stability of SNC derived from H_2SO_4. Combining XPS, FTIR, and TEM results, they confirmed the formation of sulphate esters on the surface of SNC (when using H_2SO_4) and the breakage of α-D-(1–4) and α-D-(1–6) glucosidic bonds which results in the disappearance of amorphous layers. They also pointed out that SNC's negative surface charge was due to the degradation of glucose into formic acid and levulinic acid which adsorb on SNC's surface.

3.1.2. Enzymatic hydrolysis

Amongst starch transforming enzymes one can distinguish two categories: the one that hydrolyzes glucosidic bonds, called amylase, and the one that transfer them, called transferase. Amylases are often sub-divided into 3 groups: endo-amylases, that cleave internal α(1,4) bond resulting in α-anomeric products; exo-amylases which cleave α(1,4) and α(1,6) from the non-reducing end resulting in α- or β-anomeric products; and debranching enzymes which include isoamylase and pullulanase which hydrolyze exclusively α(1,6) bonds leaving long linear polysaccharides [62]. However, they mainly found intensive use in the determination of the fine structure of amylopectin, such as reported by Angellier-Coussy et al. [63] for the study of the molecular structure of SNC. Recent publication also reports the use of enzymes for the characterization of SNC and the assessment of the DPs of polymer chains with SEC of the ensuing solution.

To our knowledge, no articles report the preparation of SNC using a purely enzymatic hydrolysis. However, an attempt has been reported by [41] rendering 500 nm particles believed to be blocklets.

Kim et al. [64] prepared starch nanoparticles by hydrolyzing waxy rice starch using α-amylase and then ultrasonicating in ethanol. The amorphous region in starch granules could be selectively removed by α-amylolysis, however it induces fragmentation in starch particles. Similarly to acid hydrolysis, the kinetic for enzymatic hydrolysis follows a two-stage profile as shown in Fig. 8. Obtained particles were 500 nm particles believed to be blocklets, and with a yield of only 5–6%. The obtained particles were unstable and thus readily swollen by physical force such as ultrasonication and thus formed starch aggregates. Hence they concluded that more precise controls in hydrolysis and recovery processes are needed. More recently, Foresti et al. [65] studied the action of alpha-amylase on waxy maize starch. They also reported a two stage kinetic of hydrolysis as observed for acid hydrolysis. Using SEM observations, they confirmed those amorphous layers were preferentially hydrolyzed during the initial high rate hours of

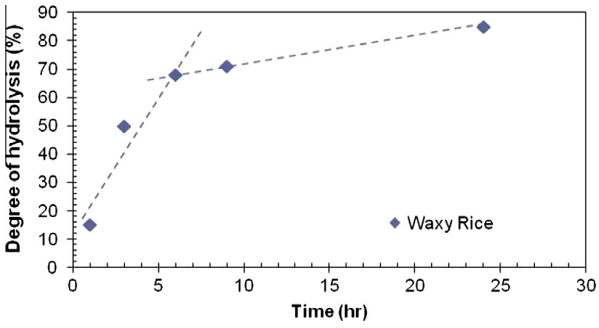

Fig. 8. Enzymatic hydrolysis profile of granular waxy rice starch. Replotted from data from Kim et al. [41].

hydrolysis. Results also showed that if the reaction was stopped after 6 h of hydrolysis, micrometric starch granules with increased crystallinity were obtained.

3.1.3. Combined enzymatic and acid hydrolysis

LeCorre et al. [66] studied the use of amylase as a pre-treatment to reduce the time of a subsequent acid hydrolysis. Amongst α- and β-glucoamylases, the latter was most efficient for producing microporous starch while keeping intact the semi-crystalline structure of starch. The hydrolysis still followed a two stage kinetic profile and within 2 h of pretreatment of waxy maize starch, the extent of acid hydrolysis reached in 24 h was reached in only 6 h (Fig. 9). The extent of acid hydrolysis reached in 120 h was reached in 45 h.

3.1.4. Using ultrasounds

Most physical treatments are expected to disrupt the crystalline structure of starch. Hence, it has been extensively studied for the production of SNP (e.g. high pressure homogenization [36]) as presented in Fig. 4. However, it has scarcely been investigated for the production of SNC.

As a contribution to the development of simple and environmentally friendly approach to preparing starch nanoparticle, Bel Haaj et al. [67] prepared starch nanoparticles using high intensity ultrasonication without additional chemicals and at low temperature of 8–10 °C in order to prevent plastization with water. Despite precaution, both XRD and Raman spectra indicated severe disruption of the crystalline structure. This was attributed to the mechanical damage brought about by high power ultrasounds (170 W). It has indeed been demonstrated [68] that ultrasonic treatment affects supramolecular structure, especially the crystalline region, as ultrasonic cavities provide more channels for water diffusion through the granule.

Kim et al. [64,69] examined the effect of milder ultrasonic treatments on nanoparticle preparation from waxy maize starch by acid hydrolysis. In the first study [64], they concluded that a mild utltrasonication once every day during the acid hydrolysis induced a higher yield of nanoparticles (<100 nm) and an additional increase in crystallinity as shown by XRD. In contrast, when the ultrasonication was performed after the hydrolysis disruption of the crystalline structure was obvious. In the following study [69], they studied the effect of applying ultrasound after cold temperature (4 °C) acid hydrolysis on yield, morphology and crystallinity. It was found that cold sulphuric acid hydrolyzed starch for up to 6 days showed similar thermal and crystalline attributes as native starch. In contrast, when the acid hydrolysis at 4 °C was performed for 6 days and followed by mild ultrasonication (identified in the previous study), an exceptional high recovery yield (nearly 80%) of nanoparticles was recovered. However, it should be mentioned that under 6 days hydrolysis, applying ultrasound to the samples resulted in particularly low crystallinity as when performed in water by Bel Haaj et al. [67].

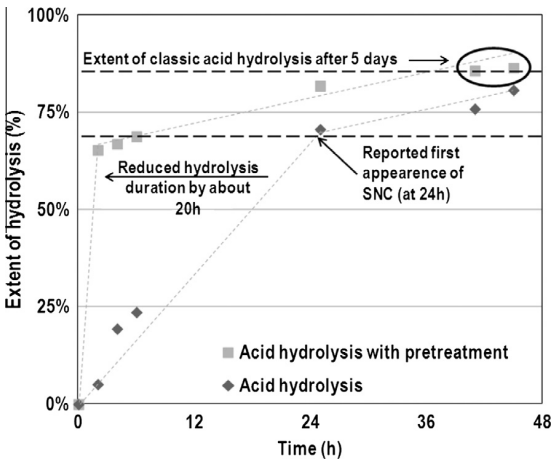

Fig. 9. Kinetics of sulphuric acid hydrolysis of (○) non-pretreated and (■) pretreated waxy maize starch. Reprinted with permission from [66]. Copyright (2010) American Chemical Society.

3.2. Regeneration

The regeneration process is most commonly used to prepare amorphous starch nanoparticles. It consists in gelatinizing the starch before "regenerating" it via a secondary process: most often solvent precipitation (as described earlier).

However, Kim and Lim [35] studied alternative ways to obtain starch nanocrystals by regeneration. They proposed a process for preparing nanoscale starch particles by complex formation (or co-crystallisation) with other components. Experiments were conducted with n-butanol. Starch was dissolved in an aqueous DMSO solution heated for 1 h and stirred for 24 h. The aliquot was passed through a PTFE 10 μm pore size membrane filter into n-butanol (3 days at 70 °C). Maximum starch precipitation was 6.78% of the initial amount. Complex formation involved mainly amylose rather than amylopectin. The precipitate (starch–butanol complex) was collected by centrifugation and washed 3 times in n-butanol. However, the complex contained a large portion of amorphous matrix, so that its selective removal by enzymatic hydrolysis was needed. Since most of the starch was hydrolyzed (85–90%), the resulting yield of the nanoparticles was extremely low. Starch nanoparticles display spherical or oval shape with diameters in the range 10–20 nm.

Most recently, Sun et al. [70] proposed a time saving regeneration method which combines enzymolysis and recrystallisation. This is the most innovative approach proposed in the last years. Contrary to Kim and Lim [35] whom first co-crystallised the starch after gelatinization and then hydrolyzed the amorphous starch; Sun et al. [70] first hydrolyze (debranches) the starch using pullulanase after gelatinization into hydrolysate with linear and low molecular weight polymer chains and then allows it to retrograde for up to 12 h to recrystallize in nanoparticles. The longer the time allowed for retrograding the smaller, the more crystalline and the more thermally stable the obtained particles. After 12 h retrogradation, nanoparticles with 30 nm diameter, 47% crystallinity and Tg = 44 °C were obtained with a yield of 55%. Needless to say that this process is highly time and yield efficient compared to the classic acid hydrolysis for producing starch nanaocrystals. A major difference does differentiate the two processes though: A change in crystalline type attributed to the reorganization of starch chains during retrogradation.

4. Properties of starch nanocrystals

Depending on the botanic origin of starch, native granules present a variety of size (2–100 μm), size distribution, shape, extraction from plant conversion factors and chemical contents [71]. Consequently, ensuing SNC differ in crystallinity, amylose content, shape, morphology, viscosity, surface activity, and thermal properties as presented in the following section.

4.1. Crystallinity

Native starches contain between 15% and 45% of crystalline material. Depending on their X-ray diffraction pattern, starches are categorized in three crystalline types called A, B and C. Imberty

and Perez [72,73] proposed a model for the double helices packing configuration to explain difference between A- and B-type starches. A-type structures are closely packed with water molecules between each double helical structure, whereas B-types are more open and water molecules are located in the central cavity formed by 6 double helices. C-type starch pattern has been considered to be a mixture of both A and B-types (Fig. 10) since its X-ray diffraction pattern can be resolved as a combination of the previous two. Another V-type was also identified as the result of amylose being complexed with other substances such as iodine, fatty acid, emulsifiers or butanol. This crystalline form is characterized by a simple left helix with six glucose units per turn [74]. This complex-formation property allows its separation from amylopectin. It led to the development of qualitative and quantitative methods to detect amylose presence or content in starch.

Contrary to cellulose nanocrystals, SNC are not almost 100% crystalline but rather 45% crystalline with variations depending on the botanic origin as presented by LeCorre et al. [75]. The degree of crystallinity remains low even after acid hydrolysis showing that an important amount of non-organized materials remains in the SNC suspension. They also found that SNC prepared by acid hydrolysis retained the same crystalline type as their native counterpart.

As described earlier, the crystallinity of starch is attributed to the packing of double helixes formed by amylopectin side chains. Therefore, amylopectin-rich starches are more crystalline than amylose-rich ones (Fig. 11a) whereas starches with similar amylose content but from different botanic origin have similar degrees of crystallinity. Similar results were found for the corresponding SNCs (Fig. 11b). Nor the crystalline type, nor only the botanic origin seem to play an important role. Consequently, the most important parameter determining the degree of crystallinity of SNC seems to be the amylopectin content.

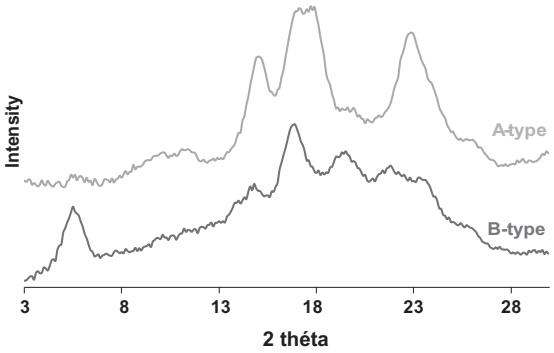

Fig. 10. Typical X-ray diffraction pattern for (a) A-type starch and (b) B-type starch.

4.2. Amylose content of starch nanocrystals

As already explained and described in Fig. 1, SNC are thought to consist in amylopectin side chains [76]. To verify the accuracy of this assumption, LeCorre et al. [75] assessed the amylose/amylopectin ratio for all starches before and after hydrolysis using the iodine binding method. It exploits the ability of iodine to stain amylose and amylopectin helixes by forming amylose-iodine complexes (V-type). The blue colour for the stain is due to the amylose component of starch. The amylopectin gives a red–purple colour which is less intense than the amylose stain. UV–VIS absorption spectra for SNC suspensions clearly differed from that of their native counter parts in that they were closer to the pure amylopectin reference.

Fig. 12 shows the correlation between absorbance at 600 nm and amylose content according to a rapid single-wave colorimetric method [77]. The amylose content of P21, M1, M27 and M70 SNC were measured to be respectively 0%, 0% (or too low a DP to be measured), 1% ± *1.8%* and 11% ± *2.1%*. Results suggested that SNC suspensions are made of low DP amylopectin.

4.3. Shape

LeCorre et al. [75] studied the influence of botanic origin on the morphology of SNC. No correlation between SNC morphology and botanic origin or amylose content was detected. Their morphology seemed rather linked to the crystalline type (Fig. 13). Indeed, waxy maize and wheat starch (A-type) rendered respectively parallelepipedic and square-like nanocrystals. High amylose maize SNC (B-type) were rather round and potato SNC (B-type) seemed to be made of both round and rounded-corner-square particles depending on size. Schematically, nanocrystals produced from A-type starches rendered square-like particles whereas nanocrystals produced from B-type starches rendered round-like particles. This could be explained by the different packing configurations of amylopectin chains for A and B-type starches, as shown in Fig. 13.

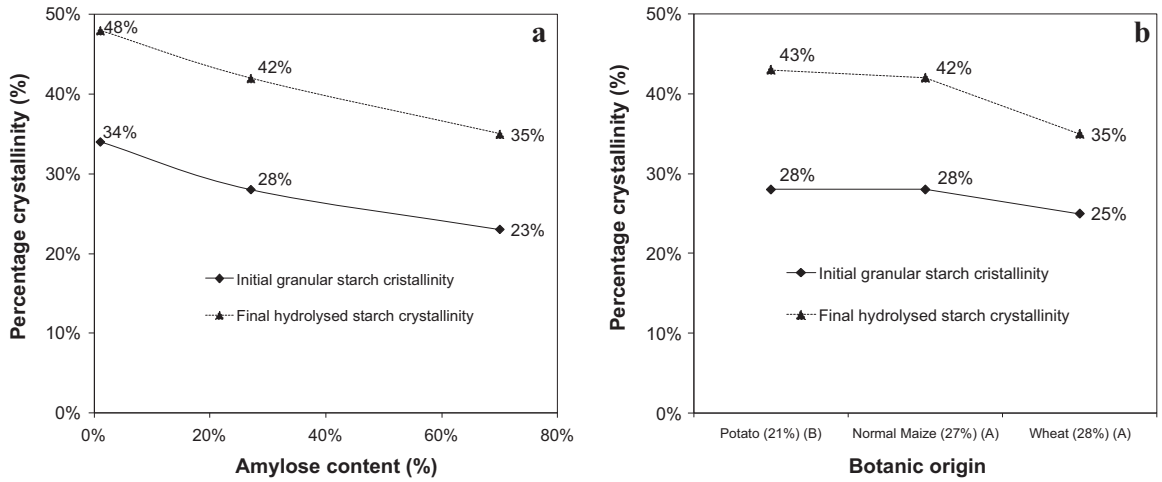

Fig. 11. Original crystallinity (plain) and final crystallinity (dot ▲) for starches with same botanic origin and different amylose content (a) and for starches with same amylose content and different botanic origin (b). From [75] *with kind permission from Springer Science and Business Media.*

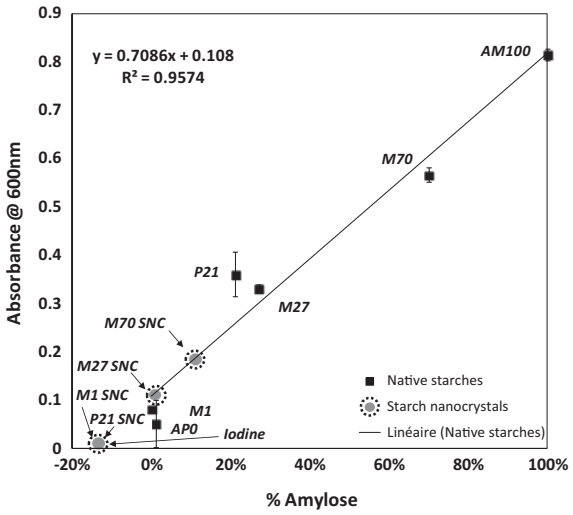

Fig. 12. Calibration graph of absorbance at 600 nm against percentage amylose for native starches. From [75] *with kind permission from Springer Science and Business Media.*

4.4. Size and thickness

Amylose molecules are thought to occur in the granule as individual molecules, randomly interspersed among amylopectin molecules and in close proximity with one another, in both the crystalline and amorphous regions [9]. Depending on the botanic origin of starch, amylose is preferably found in the amorphous region (e.g. wheat starch), interspersed among amylopectin clusters in both the amorphous and crystalline regions (e.g. normal maize starch), in bundles between amylopectin clusters, or co-crystallized with amylopectin (e.g. potato starch). Thus botanic origin should considerably influence the crystalline organization.

SNC from different botanic origin starches' size and size distributions were systematically assessed by SEM-FEG image analysis [75]. For a given botanic origin, a sliding of size distribution's main peak is observed with increasing the amylose content. This result is not surprising since amylose is believed to jam the pathways for hydrolysis (Fig. 14).

To confirm and assess the thickness of the platelet-like nanocrystals, atomic force microscopy (AFM) measurements were carried out on SNC from different origins [75] SNC were found to have thicknesses between 4 and 8 nm. This is in accordance with current models [7,63,76] which report the crystalline lamellae to be 5–7 nm and the cumulated size of crystalline and amorphous lamella to be 9–10 nm for all starches. This confirmed that SNC are individualized crystallites. No obvious relationship to amylose content (%) could be observed. Thus it seems that the thickness of SNC is rather linked to the botanic origin of starch via its internal organization (see Tables 2 and 3).

4.5. Viscosity

The rheological behaviour of SNC aqueous suspensions is important for processing. Previous work [78] has shown the influence of surface charge on cellulose nanocrystals and demonstrated that nanocrystals suspensions produced by sulphuric acid hydrolysis, contrary to uncharged ones, presented surface charges which limited time dependency (and thus thixotropic effects). LeCorre et al. [75] prepared waxy maize SNC suspensions at different concentrations and measured their viscosities. All SNC suspensions displayed a shear-thinning behaviour in the investigated shear rate range (Fig. 15). No particular relationship was found between viscosity and SNC size, thickness, surface area or specific surface.

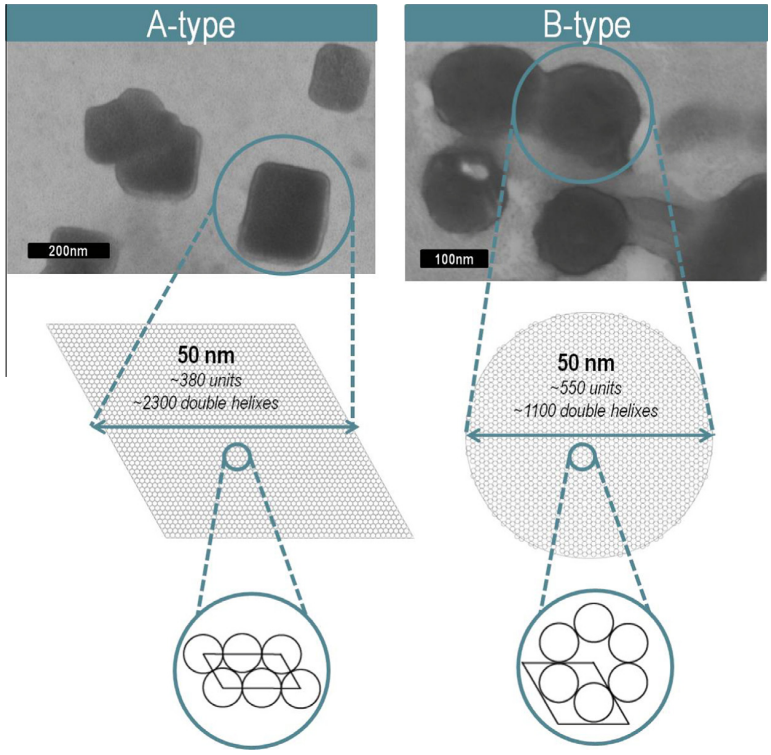

Fig. 13. Double helixes packing configuration depending on crystalline type and corresponding picture of starch nanocrystals from waxy maize starch (A-type) and high amylose starch (B-type). From [75] *with kind permission from Springer Science and Business Media.*

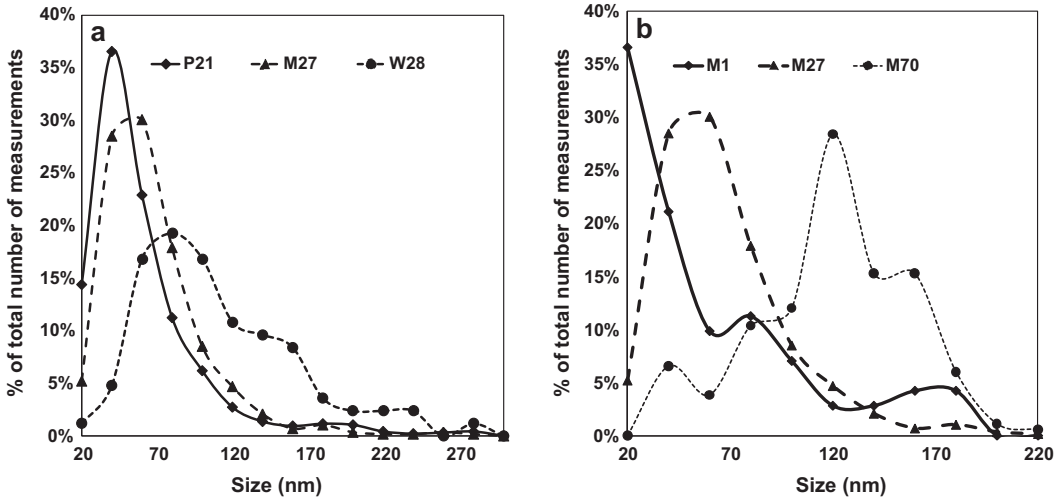

Fig. 14. Size distribution for (a) the same botanic origin and (b) the same amylose content. From [75] *with kind permission from Springer Science and Business Media.*

Table 2
Main features of native starches, and diameter and thickness of corresponding SNC. From [75] *with kind permission from Springer Science and Business Media.*

Botanic origin	Referred to as	Granular size (μm)	Amylose (%)[#]	Crystalline type	SNC diameter		SNC thickness	
					(nm)	Counts	(nm)	Counts
High amylose maize	M70	5–20	65–75	B	118 ± 53	190	5 ± 1.6[*]	76
Normal maize	M27	5–20	27	A	58 ± 36	576	8.3 ± 3.1[*]	112
Waxy maize	M1	5–20	1	A	47 ± 42	71	6.1 ± 1.9[**]	14
Wheat	W28	2–30	28	A	100 ± 50	71	3.7 ± 0.6[***]	30
Potato	P21	5–80	21	B	52 ± 4	951	7.6 ± 1.6[*]	31

[#] Supplier's data.
[*] Personnel measurements using software Gwyddon for image analysis.
[**] Conducted at «Service des Matériaux Polymères et Composites» (SMPC), Mons, Belgium.
[***] Personnel measurements on AFM software.

Table 3
Polar component ($\gamma s\ p$), nonpolar component ($\gamma s\ d$), and surface energy (γs) values of waxy maize starch nanocrystals from [60].

	γp (mJ/m^2)	γd (mJ/m^2)	γs (mJ/m^2)
SNC	30.7	31.2	61.9

However, suspensions with lowest viscosity were M70 and P21, which corresponds to suspensions with respectively disc-like morphology and ill-defined morphology (mix of square and disc) nanoparticles. Highest viscosity was achieved with wheat starch (W28) which presents square-like platelets SNC.

Fig. 15b presents the viscosity of non-crystalline starch nanoparticles (SNP prepared via reactive extrusion). It is much smaller

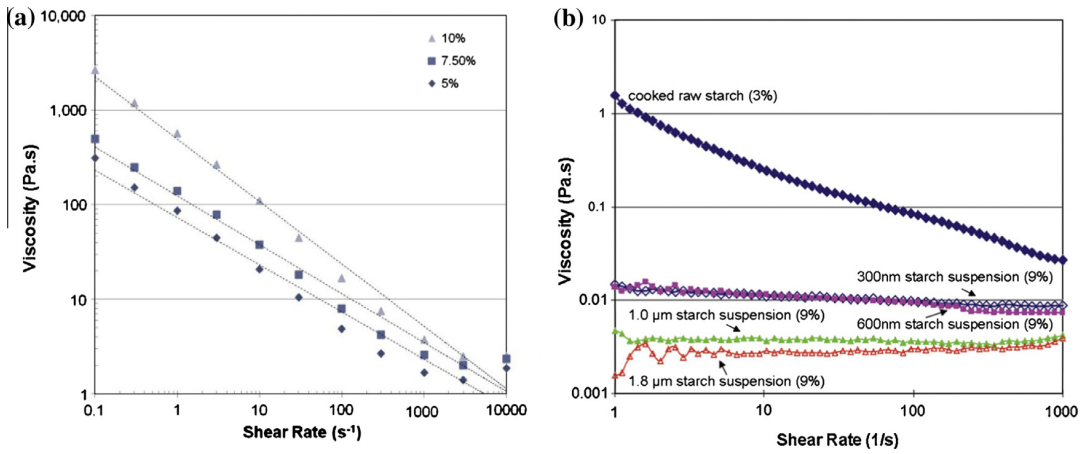

Fig. 15. Viscosity of (a) SNC from waxy maize (unpublished) and (b) starch particle suspension and cooked starch at room temperature reprinted from [120]: carbohydrate polymers, 85/1, Song et al., starch nanoparticle formation via reactive extrusion and related mechanism study, 208–214. Copyright (2011), with permission from Elsevier.

than that of SNC. This is because, for a given mass concentration, the smaller the particle, the more particles in the solution, and the higher interaction between the particles, resulting in a higher viscosity of suspension. Indeed SNC have particle size under 100 nm. Suspensions with SNP with size 600 nm or lower shows shear thinning.

4.6. Surface reactivity

Angellier et al. [79] assessed the surface properties of SNC to serve as a baseline to be compared to modified SNC prepared for nanocomposite applications. Fig. 16 illustrates that water has a high affinity for the surface of SNC. It is also clear that the decrease of contact angle values with time can be attributed exclusively to the spreading of the water drop.

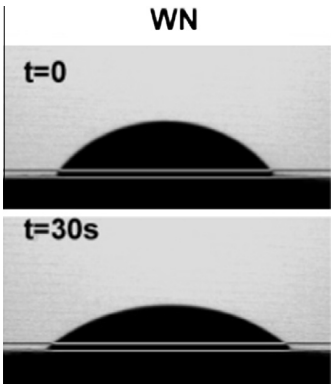

Fig. 16. Photographs of a water drop on an unmodified (WN) starch nanocrystal film surface at the moment of depositing the drops and after 30 s. From [60].

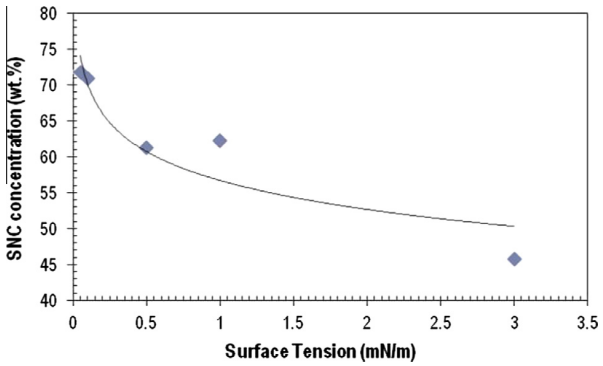

Fig. 17. Evolution of surface tension of SNC dispersion prepared in 3.16 M H_2SO_4 with starch nanocrystals content. Plotted from data from [80].

Using different solvents, the values of the polar and dispersive contributions to the surface energy were determined.

SNC particles exhibit a polar component as high as the dispersive one, as expected from an OH-rich surface. The values presented here for SNC are in agreement with those reported for similar materials and can be attributed to the high –OH content of the constituting sugar, i.e., glucose unit (3-OH groups per glucose moiety).

More recently, the surface tension of starch nanocrystal dispersion prepared in 3.16 M sulphuric acid was found to decrease from 71.7 to 45.8 mN/m when the nanocrystal concentration grew from 0.005 to 3.0 wt% [80]. Although this was to be expected, it has never been demonstrated before (Fig. 17).

These results also indicated that SNC are surface active particles which can be used to stabilise emulsions as observed in Fig. 18 [80].

4.7. Thermal properties

Starch granules thermal properties have been widely investigated [81–86] mostly using Differential Scanning Calorimetry (DSC). It detects changes in heat flow associated with first-order transitions (melting) and second-order transitions (glass transition) of polymers [87]. In excess water (Table 4), an increase in temperature leads to an endothermic peak at about 50–70 °C attributed to the gelatinization of starch. At intermediate water content (30–60%), several models have been developed to explain the two peaks generally observed: the first peak is shifted up in temperature, and a higher temperature second peak is observed. At very low water content (>20%), only the second high temperature peak is observed (Table 5).

Several physical explanations have been developed to explain these transitions: amorphous growth ring swelling [88] disrupting order and crystallinity; differences in crystallites thermal stability [89]; partial melting followed by recrystallization and final melting [90]; heterogeneous repartition of water in starch [91]; differentiated melting of crystallites and the melting of amylose lipid complexes [82].

Another approach to the understanding of starch thermal behaviour consists in considering it from a polymeric point of view, as a semi-crystalline polymer whose specific heat-temperature curves exhibit the characteristics of both glassy and crystalline polymers [87].

More recently others [86,92] have proposed a liquid–crystal approach to explain the gelatinization of starch. Side-chain liquid–crystalline polymers (SCLCP) consist of three separate components: backbones, spacers and mesogens [92] as described in Fig. 19.

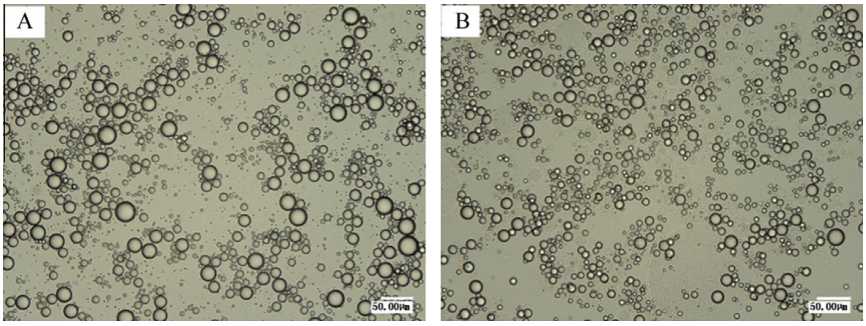

Fig. 18. Optical micrograph of the emulsion containing (A) 0.02 wt% and (B) 6.0 wt% starch nanocrystals (scale bar 50 mm). Reprinted from [80] carbohydrate polymers, 64/6, Song et al., emulsion stabilized by starch nanocrystals, 497–502. Copyright (2012), with permission from Elsevier.

Table 4
Characteristic temperatures observed for the endothermic transitions of starches and corresponding SNC in excess water (starch: H20 30:70). From [75] *with kind permission from Springer Science and Business Media.*

			NATIVE				NANOCRYSTALS							Comparison
Starch type	WC (%)		Ti (°C)	Tmax (°C)	Tf (°C)	Range Δ (°C)	Ti (°C)	±	Tmax (°C)	±	Tf (°C)	±	Range Δ (°C)	Shift of peak (°C)
M70	70	P1	69.1	72.5	78.3	9.2	84.5	12.5	93.0	2.1	99.9	1.0	15.4	20.5
		P2					106.7	6.3	103.1	3.5	112.9	5.2	6.2	
M27	70	P1	63.9	69.4	81.9	18.1	67.6	2.2	85.5	1.3	99.7	0.5	32.1	16.1
		P2					100.2	0.1	106.6	2.1	112.9	3.2	12.8	
M1	70	P1	65.0	71.4	83.4	18.4	54.5	14.9	79.7	11.6	99.2	0.3	44.7	8.3
		P2					99.9	0.5	104.0	1.6	108.6	0.8	8.6	
W28	70	P1	53.3	59.1	76.4	23.1	59.0	9.1	77.7	11.8	100.7	1.7	41.8	18.6
		P2					101.7	1.1	105.5	0.3	111.3	2.2	9.6	
P21	70	P1	59.6	64.0	82.5	22.9	82.1	10.2	91.3	4.3	100.3	0.5	18.2	27.3
		P2					101.6	0.4	105.5	0.1	110.0	1.6	8.4	

Ti: onset temperature, Tmax: maximum peak temperature, and Tf: final temperature.
P1: first endothermic peak and P2: second endothermic peak.

Table 5
Characteristic temperatures observed for the endothermic transitions of starches and corresponding SNC in the dry state (50%RH conditioning). From [75] *with kind permission from Springer Science and Business Media.*

			NATIVE				NANOCRYSTALS							Comparison
Starch type	WC (%)		Ti (°C)	Tmax (°C)	Tf (°C)	Range Δ (°C)	Ti (°C)	±	Tmax (°C)	±	Tf (°C)	±	Range Δ (°C)	Shift of peak (°C)
M70	0	P1					116.0	2.2	148.3	2.8	178.2	2.5	62.1	25.7
		P2	94.6	122.6	231.1	136.5	193.3	3.3	205.4	3.8	246.0	0.5	52.6	
M27	0	P1					105.0	7.8	126.1	6.3	161.0	0.2	56.0	−22.6
		P2	109.6	148.7	255.0	145.4	247.2	1.4	253.5	1.0	256.9	0.0	9.7	
M1	0	P1					123.4	11.2	154.0	2.2	180.3	10.2	56.9	29.3
		P2	107.6	124.7	223.5	115.9	188.0	9.1	200.0	10.2	234.0	7.4	46.0	
W28	0	P1					186.6	2.5	199.0	9.3	212.8	12.0	26.2	68.3
		P2	104.8	130.7	241.4	136.6	215.9	13.2	218.9	12.6	248.3	6.4	32.4	
P21	0	P1					178.9	3.0	191.4	9.2	205.4	23.1	26.4	43.8
		P2	111.6	147.6	204.8	93.2	207.0	21.7	215.3	9.7	245.5	5.6	38.4	

Ti: onset temperature, Tmax: maximum peak temperature, and Tf: final temperature.
P1: first endothermic peak and P2: second endothermic peak.

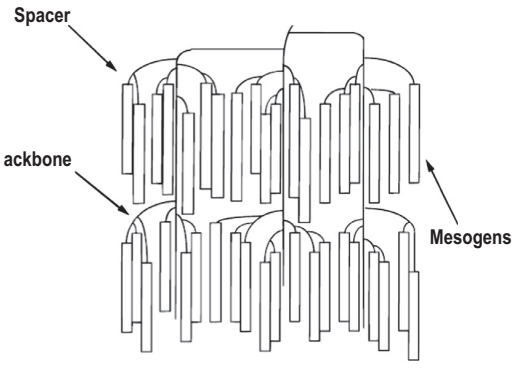

Fig. 19. Illustration of the SCLCP potential of amylopectin side chain clusters. Adapted from with permission from [125]. Copyright (1998) American Chemical Society.

Mesogen is the fundamental unit of a liquid crystal that induces structural order in the crystals. The double helices of the amylopectin side chains correspond to mesogens, which are attached to the backbones by short spacer units (connecting points). Considering the SCLCP nature of amylopectin, Waigh et al. [86] and Atichokudomchai et al. [85], described, as presented in Fig. 20, a first thermal transition corresponding to a smectic (lamellar order)/nematic (orientationally ordered) transition for B-type starches, and to a nematic/isotropic phase transition for A-type starches (ie. helix-helix dissociation). They also attributed the second transition to a helix-coil transition (ie. unwinding of double helices to a gel phase). In excess water (>60%) (Fig. 20a), the difference between the two endotherms is immeasurably small and are thought to occur almost simultaneously. At intermediate water content (30–60%) (Fig. 20b), the two endotherms can be evidence one after the other. In low water content (<30%) (Fig. 20c), a direct glassy-nematic (or crystalline) to gel transition occurs as the helices unwind for B and A-type crystallinity respectively (one peak).

Two different processes are shown for A and B type starches: in B-type starch the intermediate phase is nematic in character, and in A-type starch the intermediate phase is isotropic in character; and (c) in very low water content. It is proposed that the intermediate phase is determined by the length of the amylopectin helices. Relative values of the orientational (φ), lamellar (ψ), and helical order parameter (h) are included. Adapted from [86].

Reports on the thermal behaviour of SNC is scarce in literature. Thermal behaviour data for freeze-dried waxy maize SNC was reported by Angellier to observe the plasticizing influence of water, and by Thielemans et al. to compare with grafted SNC. The first author [60] reported the existence of two endothermal peaks in excess water with a broad temperature range, and the

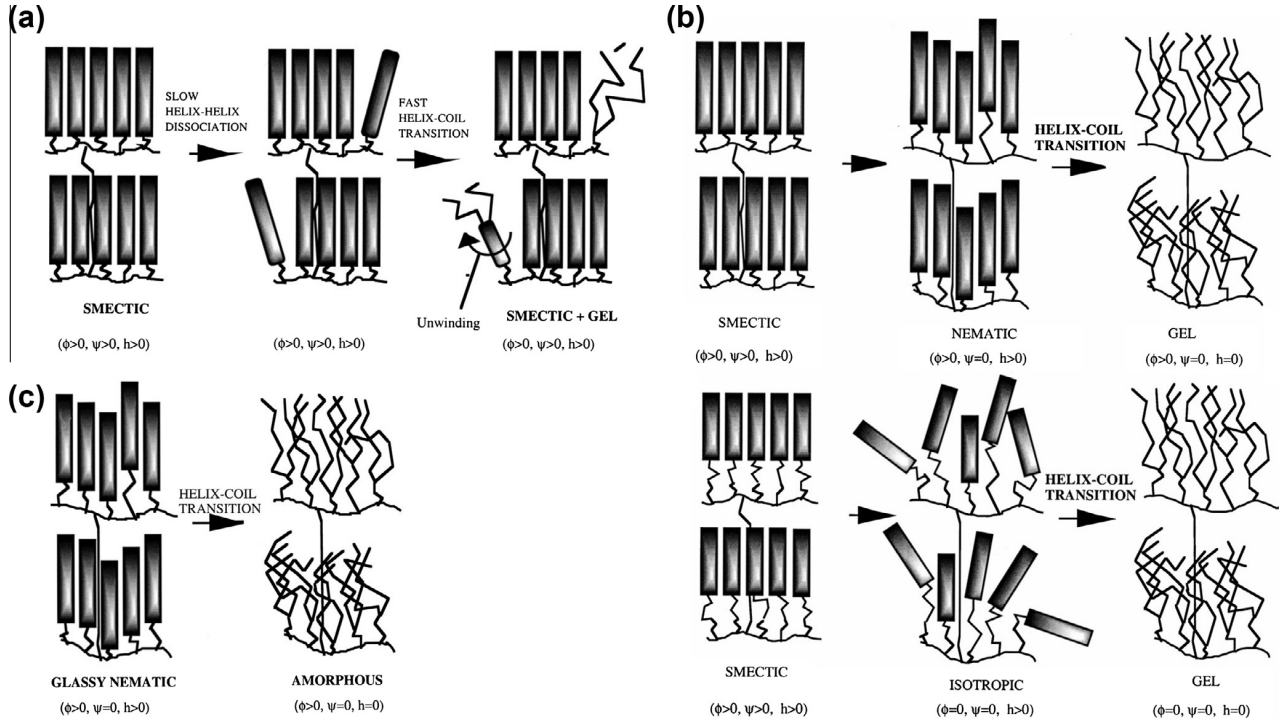

Fig. 20. Processes involved in the gelatinisation of starch in (a) excess water, (b) limiting water and (c) very low water content. In limiting water (b), two different processes are described for A and B-type starches. In B-type starch the intermediate phase is nematic whilst in A-type starch the intermediate phase is isotropic. It is proposed that the intermediate phase is determined by the length of the amylopectin helices. Adapted from [86]. Copyright (2012), with permission from Elsevier.

disappearance of the first peak in the dry state. The other authors [93] presented a DSC thermogram for waxy maize SNC in dry conditions for comparison and evidencing of grafting. The thermogram for freeze-dried SNC also showed two endothermic peaks. The first maximum peak is located around 150 °C and the second one around 200 °C. No explanation was provided. Also, no data was found concerning SNC from other sources.

Investigation of the thermal properties of SNC from different sources by DSC revealed two thermal transitions, contrary to native starches which show only one transition. Typical responses are presented in Fig. 21a in excess water and Fig. 21b in dry state. The thermal behaviour of each kind of particles, i.e. starch granules and SNC is explained and detailed in LeCorre et al. [94].

In excess water, the first peak was attributed to the first stage of crystallites melting (unpacking of the double helixes) and the second transition to the second stage of crystallites melting (unwinding of the helixes). B-type crystallinity SNC "gained" more stability than A-type SNC as they consist of more rigid crystallites.

In the dry state, the peaks were attributed to crystallites melting, with a direct transition from packed helixes to unwinded helixes; and the presence of two peaks was attributed to heterogeneity in crystallites quality.

It was demonstrated by TGA measurements (Fig. 22) that the second peak occurred before depolymerization and corresponded to the theoretical values of perfect crystallites melting.

It confirms that SNC are individualized crystallites with small polymer chain length and high melting temperature. It was also noted that differences between starches observed in the native state are somewhat compensated when in SNC. However, it seems that in excess water B-type crystallites (with longer chain length)

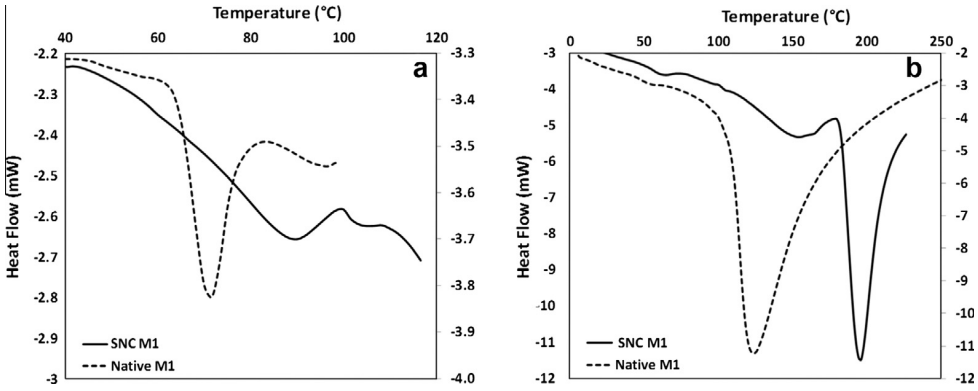

Fig. 21. DSC thermograms for native and SNC from M1 (a) in excess water and (b) in the dry state (0%WC, 50%RH conditioning) Reproduced from [94]. Copyright (2012), with permission from Elsevier.

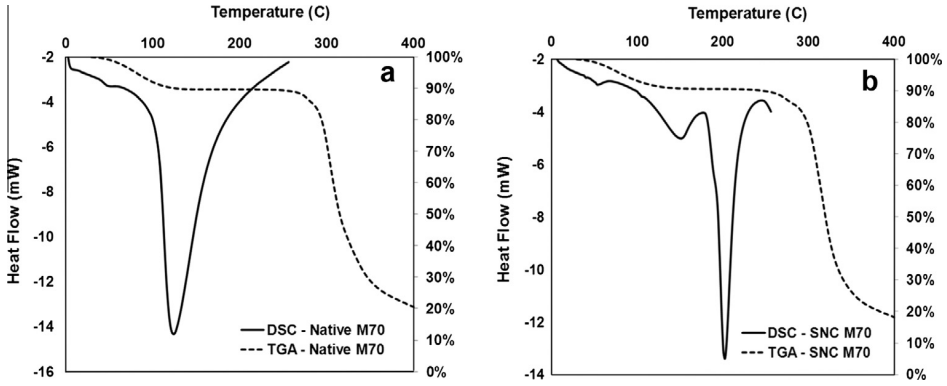

Fig. 22. DSC and TGA curves for dry (0%WC, 50%RH) (a) native M70 and (b) M70SNC. Reproduced from [94]. Copyright (2012), with permission from Elsevier.

are more stable and that in dry conditions, maize SNC showed least homogeneous crystallites. In summary, SNC can be used in wet processes, such as coating, if temperature remains lower than 80–100 °C, and in dry processes at temperatures below 150–200 °C.

4.8. Biodegradability

Kümmerer et al. [95] studied the biodegradability of organic nanoparticles in the aqueous environment via the OECD's standardized procedure of the close bottle test (CBT). SNC showed significantly faster degradation in the first 7 days than was recorded for macroscopic starch and cellulose whiskers. After 28 days, SNC reached a degradation percentage of 60% which is the excluded limit defined by the OECD for biodegradability. For comparison cellulose whiskers reached 53% and carbon nanotubes (CNT) and fullerene did not degrade at all. Furthermore, none of the particles were found to be toxic to micro-organisms necessary for oxygen take-up.

5. Modification of starch nanocrystals

Because one of the main application of SNC is in nanocomposites, there has been a growing interest towards modified SNC as it is an interesting option for improving compatibility with apolar polymer matrices [96,97] or for allowing the use of dry processes [98] since nanofillers can agglomerate in the dry state. Different routes of surface chemical modification of starch nanocrystals have been extensively studied, including mainly the grafting of small molecules or polymer chains, but also cross-linking reactions.

5.1. Grafting

Two recent review articles [99,100] have focused their attention on the processing of SNC for nanocomposites applications. Dufresne [99] extended his review to polysaccharide nanocrystals and focused on nanocomposites' transformation into a co-continuous material. Lin et al. [100] overviewed the starch nanocrystal's reinforced polymers with emphasis on methods and strategies for chemical modifications. Starch nanocrystals possess a reactive surface covered with numerous active hydroxyl groups which provide the possibility of chemical modification. Considering nanocrystals with uniform geometrical dimensions, the content of active hydroxyl group on the surface of the nanocrystal can be calculated [60] and is estimated to be ca. 0.0025 mol g^{-1} of the total amount available.

Common chemical modifications of starch nanocrystals are represented in Fig. 23 and have been reviewed in detail by Lin et al. [101].

There are mainly three strategies for chemical modification of SNC: (i) modification by chemical reaction with small molecules, (ii) "grafting onto" polymer chains with coupling agents (Fig. 24), and (iii) "grafting from" polymer chains with polymerization of a monomer (Fig. 24) [102].

Angellier et al. [79] first reported the study of functionalization, by **chemical reaction** of SNC to broaden the number of possible polymeric matrices by allowing the processing of composite materials from an organic solvent (instead of aqueous suspensions). The chemical modification consisted in transforming the polar hydroxyl group sitting at the surface of SNC into moieties capable of enhancing interactions with non polar polymers. Studied reactions were: esterification with an anhydride function and urethane formation using isocyanate. In a recent study by Xu et al. [103], acetylated SNC were prepared to improve their solubility in organic solvents such as acetone, chloroform and ethyl acetate. Solubility and turbidity were assessed visually. Peculiar observation of change of crystalline type from A to V was reported with increasing DS values. Also, platelet like starch nanocrystals became sphere-like shaped after modification and their size increased from 20–40 nm to 63–271 nm.

Thielemans et al. [93] studied the "**grafting onto**" approach with longer-chain surface modification for forming directly a polymer matrix phase at the nanocrystals surface or at least for achieving near-perfect stress transfer between matrix and reinforcement thanks to strong covalent linkages. Two modifications were studied: stearate grafting and polyethylene glycol methyl ether (PEGME) modification via TDI. In continuation of that work, Labet et al. [104] reported the grafting of PTHF, PPGBE and PCL. Most recently, Wang et al. [105], synthesized SNC-g-polystyrene via free radical emulsion copolymerization. Partial grafting of SNC with conservation of crystalline properties was reported in all studies. However, the "graft onto" approach clearly changes the characteristics of SNC such as morphology (as shown in Fig. 25), size, polarity, dispersion in organic solvent, surface and thermal properties.

The following studies considered a "**grafting from**" approach. Song et al. [106] prepared amphiphilic SNC by free radical polymerization (FRP) to allow the substitution of carbon black by SNC as a green filler of natural rubber at high filler content. In this study, styrene graft copolymerization was undertaken to introduce hydrophobic groups or polymer chains onto the polysaccharide backbone. Namazi and Dadkhah first studied the SNC grafting with PCL via classic ring opening polymerization (ROP) [107] and more recently [22] reported a method for preparing hydrophobically modified SNC using fatty acid. In contrast with work using heterogeneous reaction conditions, their interest was focused on homogeneous reactions by taking advantage of SNC specific area. Others [108] developed also this ROP

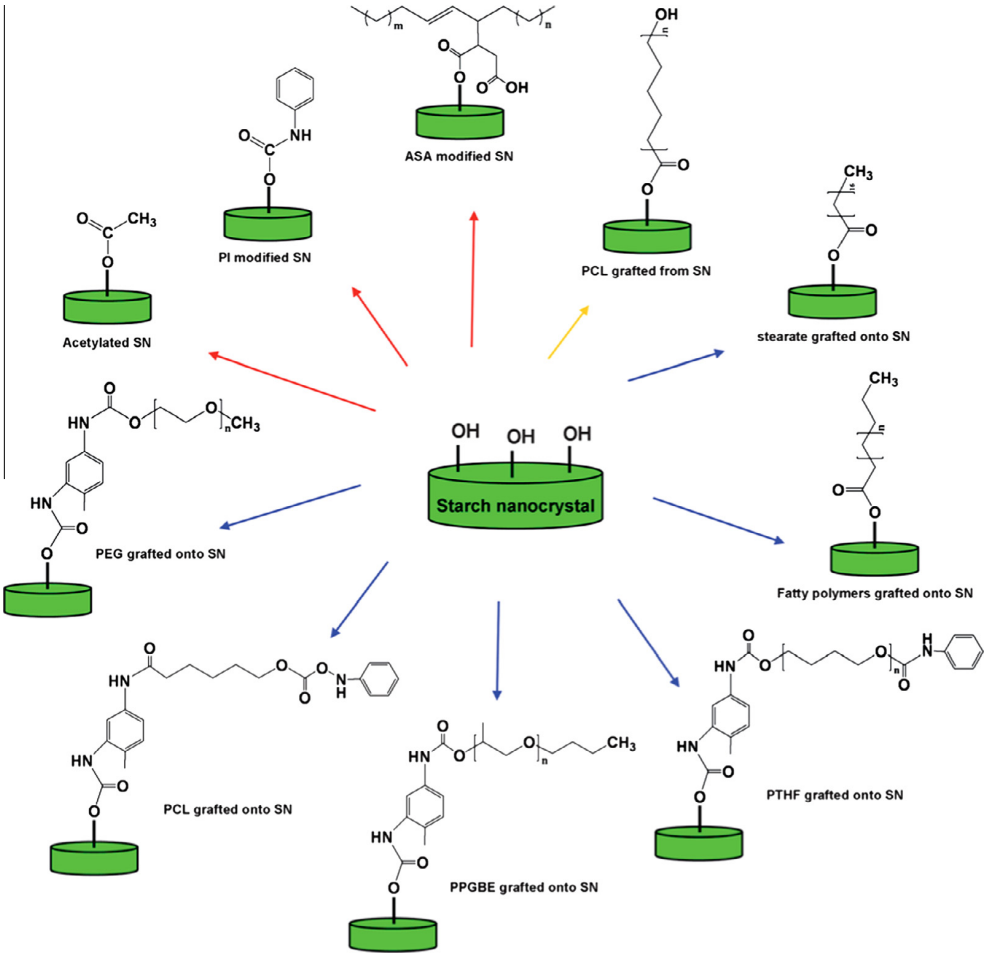

Fig. 23. Common chemical modifications of starch nanocrystals. From [101] – reproduced by permission of The Royal Society of Chemistry.

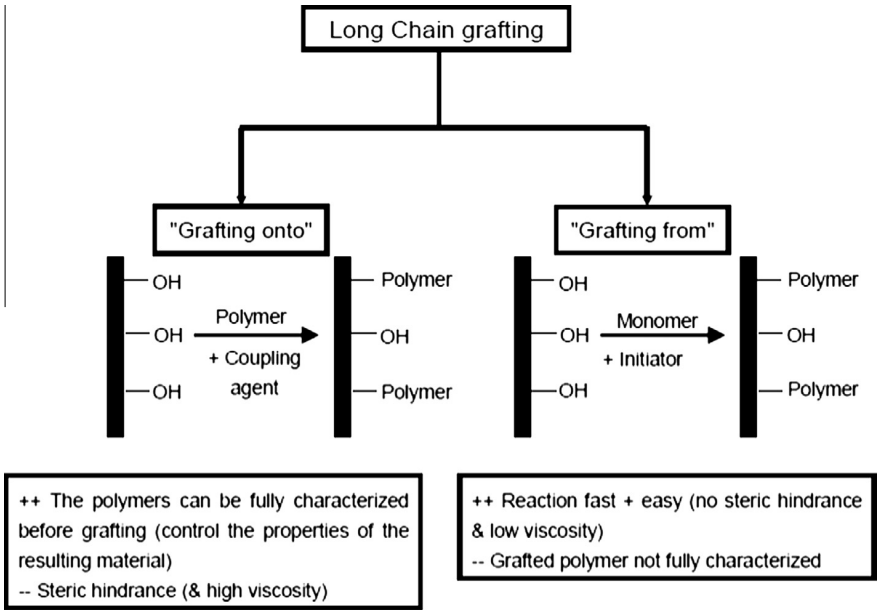

Fig. 24. Schematic representation of the "grafting onto" and "grafting from" approaches. From [99].

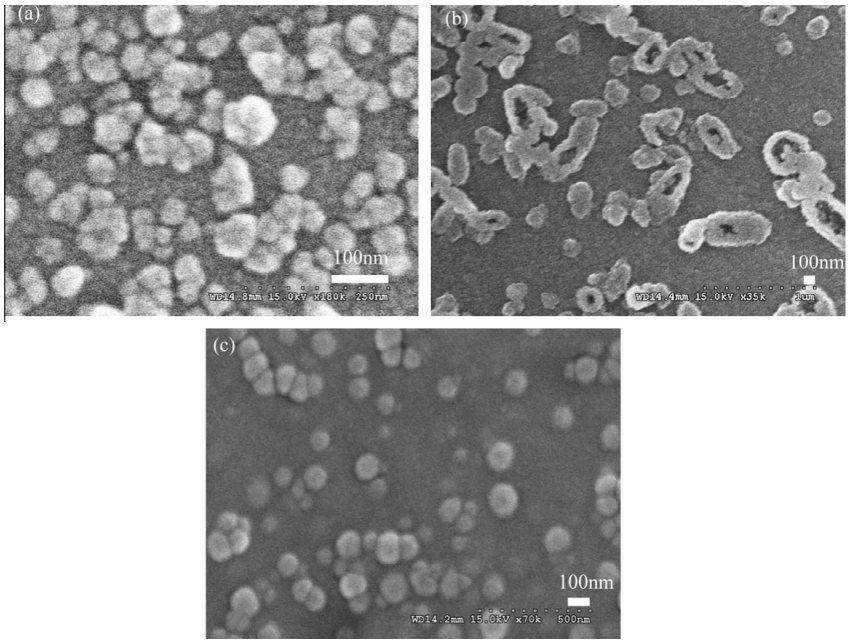

Fig. 25. Morphologies of starch nanocrystals and starch nanocrystals-g-polystyrene of different reaction time (a) ungrafted starch nanocrystals, (b) StN-g-PS sample B1 of 5 h, GR 6.42%, and (c) StN-g-PS sample B2 of 8 h, GR 17.98%. From [105]. Copyright © 2014 Wiley Periodicals, Inc.

treatment for an extrusion process application. Yu et al. [19] and Chang et al. [109] used microwave to graft SNC with polycaprolactone. They showed that PCL-modified SNC retained their morphology [19]. The crystallinity was also retained but thermal decomposition occurred over a broader range of temperatures.

5.2. Cross-linking

To improve the re-dispersibility of SNC prepared by acid hydrolysis, Ren et al. [110] have proposed a simple cross-linking method. SNC were prepared according to Angellier et al. [50]. Then SNC suspension was diluted and redispersed for 30 min at 40 °C using ultrasounds (600 W); after which the cross-linker (Sodium hexametaphosphate, SHMP) was added and the pH adjusted. The reaction was allowed to occur over 4 h. The crystalline structure of the cross-linked SNC was not disrupted, and their dispersion was significantly improved.

Jivan et al. [111] proposed to cast light on water redispersible SNC developed by Ren et al. [112]. Cross-linked SNC formed a significantly stronger lattice than their unmodified counterpart and thus showed high thermal stability (no phase transition up to 150 °C).

It should also be noted that cross-linking is also used for the preparation of starch nanoparticles (not nanocrystals). Ma et al. [33] prepared starch nanoparticles by precipitating a starch solution within ethanol as the precipitant followed by cross-linking with citric acid. Most recently, Yang et al. [113] have prepared nanoparticles by cross-linking a reversed-phase starch microemulsion.

6. Application of starch nanocrystals in the field of nanocomposites

Starch nanocrystals, produced from bio-sourced and renewable resources, appear as promising candidates for improving mechanical, barrier and also electrical properties of polymer matrices in light of their platelet-like shape and their ability to establish both a percolating network and interactions with the polymer matrix. Since starch nanocrystals are initially available in the form of aqueous suspensions, starch nanocrystals-based nanocomposites are mainly prepared by casting and water evaporation, from either polymer latexes, hydro-soluble or -dispersible polymers. By the way, starch nanocrystals were first used as reinforcements in elastomer-based latexes such as poly(styrene-co-butyl acrylate) [114] and natural rubber [126–129]. Since 2006, most of the work has been oriented toward the use of bio-sourced and/or biodegradable hydro-soluble or hydro-dispersible polymers such as waterborne polyurethane [17,109], starch [131–134], pullulan [135], soy protein isolate (SPI) [136] and carboxymethyl chitosan [137].

The main hurdle of starch nanocrystals is their hydrophilicity, restricting their use as a reinforcing phase in hydrophilic polymers. Hence, as described in Section 5, different routes of surface chemical modification of starch nanocrystals have been extensively studied to improve the affinity between the filler and hydrophobic polymer matrices. The amphiphilic nature imparted upon polysaccharides after hydrophobic modification provides them a wide and interesting applications spectrum, for instance as rheology modifier, emulsion stabilizer, surface modifier, and as drug delivery vehicles. Considering here the field of nanocomposite applications, starch nanocrystals have been tested as reinforcing fillers in poly acid lactic (PLA) [19], polyvinyl alcohol (PVA) [18] and poly(butylene succinate) (PBS) [138]. In that case, alternative processing methods consist in freeze-drying aqueous suspensions of starch nanocrystals, and subsequently mixing them with the polymer by using an appropriate (with regard to the matrix) organic solvent or, in a very less extent, extruding and hot-pressing the mixture. Morphological analysis highlighted that the dispersion state of starch nanocrystals was strongly related to the filler content, which was proved to impact the functional properties of nanocomposites.

6.1. Preparation of starch nanocrystals-based nanocomposites

Two different cases can be distinguished according to the nature of the polymer matrix. The first case corresponds to aqueous systems and regroups polymer latexes, hydro-soluble or hydro-dispersible polymers. The second case corresponds to non-aqueous systems, for which the use of organic solvent is required.

In all the studied systems, it is generally demonstrated by wide-angle X-ray diffraction analysis that the conditions used to prepare nanocomposites allowed the preservation of the crystalline structure of starch nanocrystals. Regardings the morphology of nanocomposites, it is largely demonstrated by either AFM analysis or SEM observations that increasing the content of starch nanocrystals favours their agglomeration, and thus the formation of large domains within the polymer matrix, in detriment of the improvement of functional properties.

6.1.1. Polymer latexes, hydro-soluble or -dispersible polymers

Starch nanocrystals were first used as reinforcements in elastomer-based latexes such as poly(styrene-co-butyl acrylate) [114,139] and natural rubber [126–129]. More recently, other latexes such as polyvinyl alcohol (PVA) [137] and waterborne polyurethane [17,109] were used. In that case, the basic procedure to prepare nanocomposites consists in (i) mixing an aqueous suspension of starch nanocrystals and a polymer-based latex, generally under magnetic stirring, (ii) vacuum degassing to avoid the formation of bubbles during water evaporation and thus, heterogeneities in the final films, and (iii) latex film formation by casting and water evaporation above the glass transition temperature of the polymer (Fig. 26). The formation of a latex film arises from the coalescence of the individual latex particles (i.e. concentration and compaction, deformation, cohesion and polymer chain inter-diffusion), which are normally held apart by stabilising forces. Three stages can be distinguished. In the first stage of water evaporation from the latex surface, the solid content in the medium increases and the latex particles get closer. The second stage starts when the system is sufficiently concentrated and the particles come into irreversible contact. The soft polymeric particles deform and adopt a polyhedral form. Finally, when a continuous film is formed, the remaining water leaves the film initially via any remaining interparticle channels and then by polymer chain diffusion through the fused polymer skin. Boundary between the former particles disappears leading to a continuous polymer film containing the dispersed starch nanoparticles (Fig. 26).

This route of processing allows preservation of the individualized state of the nanoparticles resulting from their colloidal dispersion in water, for starch nanocrystals contents from 2 wt% up to 50 wt%. The stability of the aqueous starch nanocrystals suspensions, and consequently the homogeneity of the resulting nanocomposite films, depends on the dimensions and surface charge of the dispersed starch nanocrystals. For example, it was shown that the use of sulphuric acid led to more stable aqueous suspensions than those prepared using hydrochloric acid, due to the formation of negatively charged surfaces [114]. Indeed, during acid hydrolysis via sulphuric acid, acidic sulphate ester groups may probably be created on the nanoparticle surface, creating an electric double layer repulsion between the nanoparticles in suspension.

A similar processing route is generally preferred for hydro-soluble or -dispersible polymers such as starch [131–134], pullulan [135], soy proteins [136], or carboxymethyl chitosan [137], by mixing an aqueous suspension of starch nanocrystals and an aqueous suspension or solution of polymer. The ensuing mixture is generally evaporated to obtain a solid nanocomposite film. But it can also be freeze-dried to obtain nanocomposite powders, which are further extruded and/or hot-pressed, as described by Zheng et al. for soy proteins based systems [136]. For all these polymers, the use of plasticizers such as glycerol or sorbitol is often required to impart film flexibility.

6.1.2. Non-aqueous systems

In the case of polymers that are only dispersible or soluble in organic solvents, powders of freeze-dried starch nanocrystals are dispersed in an organic solv ent, appropriately chosen according to the considered polymer matrix, e.g. trichloromethane in the case of PBS [138] or dichloromethane for PLA [19]. Then, as previously described for aqueous-based systems, the two solutions/suspensions are mixed. The resulting mixture is cast and the solvent is evaporated to obtain solid nanocomposite films. The challenge here is to reduce the surface energy of starch nanocrystals in order to improve their dispersibility and compatibility with non-polar media. For that purpose, the surface chemical modification of starch nanocrystals, as previously described in Section 5, is a strategy often considered.

6.2. Mechanical properties

The reinforcing effect of starch nanocrystals has been evaluated both in the linear range using dynamic mechanical analysis (DMA) and in the non-linear range through tensile tests. This section discusses the reinforcing effect of starch nanocrystals, the influence of surface modification on this reinforcing effect, as well as the mechanisms proposed to explain it.

6.2.1. Reinforcing effect of starch nanocrystals

Dufresne and Cavaillé [139] were the first to report the reinforcing effect of starch nanocrystals in an elastomer-based matrix, especially in the rubbery state as demonstrated by DMA experiments. For instance, the relaxed modulus at the rubbery plateau of a poly(styrene-co-butyl acrylate)-based film containing 30 wt % of potato starch nanocrystals was 100 times higher than that of the matrix [139]. In the case of a natural rubber matrix, Angellier et al. [126] reported an increase in the relaxed storage modulus of 10%, 75% and 200% for 10, 20 and 30 wt% of waxy

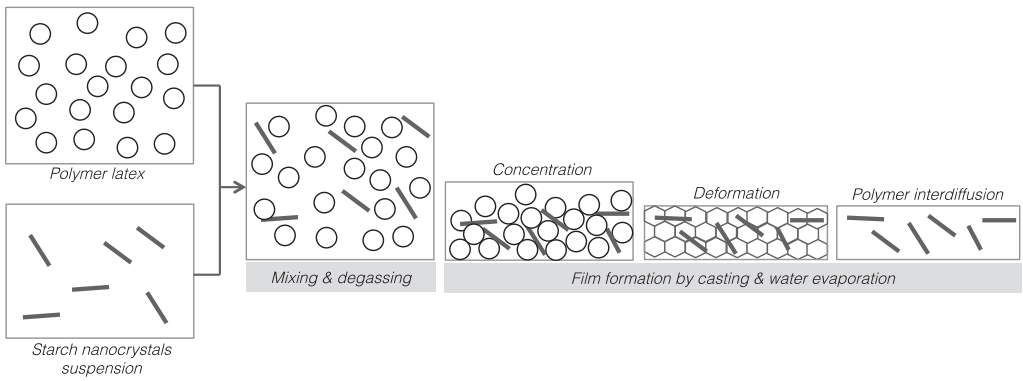

Fig. 26. Preparation of starch nanocrystals-based nanocomposite films from polymer latexes.

maize starch nanocrystals, respectively. In both cases, no increase of the main relaxation temperature associated to Tg was observed, which was an indication of poor adhesion between the filler and the elastomer-based matrix [126,139]. Most authors further confirmed the reinforcing effect of starch nanocrystals for other types of matrices, such as thermoplastic starch [132–134], pullulan [135] and soy protein isolates [136]. In the case of thermoplastic starch either plasticized with glycerol [128,134] or sorbitol [131]. The increase in filler content led to a shift of the main relaxation process toward higher temperatures (from 3 °C for the unfilled matrix plasticized with 25 wt% of glycerol to 39.8 °C for the same material filled with 15 wt% starch nanocrystals) due to a reduction of the mobility of amylopectin chains [134]. This demonstrates the presence of interactions between the filler and the matrix due to hydrogen bonding forces. This was attributed to filler/matrix interactions, was also obtained for pullulan [135] and waterbone polyurethane matrices [17]. However, in the case of WPU matrix, no reinforcing effect of starch nanocrystals was recorded by DMA experiments [17].

The reinforcing effect of starch nanocrystals was also evidenced from tensile tests in the non-linear range. Relative values of Young modulus, strength (or stress at break) and strain at break reported by different authors are collected in Table 6 for comparison. For most authors, the introduction of starch nanocrystals resulted in the increase of both the relaxed storage modulus and the stress at break, with a decrease in the strain at break [126,131,134–137].

In the case of natural rubber, considering the ultimate properties, a good compromise between the increase of the strength and the decrease of the elongation at break seemed to be reached for a filler content around 20 wt% [126]. The tensile modulus increased nearly exponentially with filler content, from 0.64 MPa for the neat matrix up to 77.8 MPa for nanocomposite films filled with 30 wt%. These values are lower than the storage tensile modulus values reported from DMA experiments (respectively 1.28 and 257 MPa) at room temperature. Given that in DMA analysis the adhesion between the filler and the matrix is less involved than in tensile tests because of weaker stresses applied, this result confirms a lack of intimate adhesion between both components of the composite structure [126].

In conclusion, starch nanocrystals represent a good substitute to carbon black, which is for the moment the most important reinforcing agent used in the rubber industry (in particular for tire applications) in spite of its fossil origin, non-biodegradability and black colour. This is further supported by the study of Angellier et al. [126] showing that the addition of only 10 wt% of SNC to NR induces a reinforcing effect (in terms of stiffness) similar to the one observed with 26.6 wt% of carbon black, while the elastic behaviour of NR-based composites is preserved, even for high starch nanocrystals contents, contrarily to carbon black [126].

In the case of thermoplastic starch as matrix, the particularly drastic decrease in the strain at break may be explained at least partially by the filler/matrix interactions which were evidenced by DMA tests [131,134,135].

In the case of a protein-based matrix, a filler content of 2 wt% seemed to be the optimal content, with the highest strength and Young modulus [136]. With increasing pea SNC content, the strength and Young modulus gradually decreased, but almost all nanocomposites kept higher resistance and rigidity than the neat matrix. However, the addition of pea starch nanocrystals caused the decrease of the elongation at break. The reinforcement for low-starch nanocrystal loading level was most likely attributed to the uniform distribution of starch nanocrystals as stress-concentrated point in SPI matrix. On the contrary, starch nanocrystals used at a higher content easily self-aggregated as large domains, which decreased the effective active starch nanocrystal surface for interacting with the SPI matrix [136]. Such behaviour was similarly observed for carboxymethyl chitosan reinforced systems [136].

The reinforcing effect of either potato or pea starch nanocrystals in a WPU matrix was investigated in two studies conducted by the same research team [17,130]. For low filler contents (up to 8 wt% only), all the nanocomposites displayed better mechanical properties than the neat WPU matrix, with a simultaneous enhancement in strength, Young modulus and elongation at break [17]. This was attributed to the uniform dispersion of starch nanocrystals at the nano-scale as well as to interfacial interactions between starch nanocrystals and the WPU matrix. However, a lower enhancement in elongation at break was noted for filler contents higher than 2 wt%, whereas a lower increase in both Young modulus and strength was noted for filler contents higher than 5 wt%. It was shown by wide angle X-ray analysis that self-aggregation of starch nanocrystals occurred with increasing loading levels, leading to the break of the original structure and interactions, and even causing severe microphase separation between pea starch nanocrystals and WPU matrix [17]. In the study of Zou et al. [130], the sedimentation and self-aggregation of pea starch nanocrystals was inhibited, leading to great enhancement of both the stress at break and Young's modulus of the nanocomposites for filler contents up to 30 wt% whereas about 300% of elongation was maintained in materials (Table 6). Herein, the system containing 10 wt% of starch nanocrystals had the maximum stress at break and an enhanced Young's modulus that were ca. 2.7- and 37-folds over those of neat WPU, respectively. The nanocomposite containing 30 wt% of starch nanocrystals had the highest Young's modulus, which was enhanced by about 67 folds. The prominent improvement of mechanical performance was attributed to the enduring stress of the rigid filler and stress transfer mediated by strong interactions between pea starch nanocrystals and the WPU matrix [130]. It was concluded by authors that such work rendered a strategy for achieving high mechanical performance of waterborne polyurethane-based nanocomposites by a simple method, and the novel bionanocomposites developed could have great potential applications, for example in the field of leather and textile finishing, floor coverings, or adhesives.

A little but significant simultaneous enhancement of the strength, toughness and rigidity was also observed for PBS filled with pea starch nanocrystals loadings up to 5 wt% [138]. For filler contents higher than 5 wt%, only the Young modulus was improved. As already mentioned for SPI and WPU matrices, the incorporation of large amounts of nanofiller (above the percolation threshold) may lead to self-aggregation and separation between the starch nanocrystals phase and the PBS matrix. This decreases the effective active nanofiller surface available for interaction with the PBS molecules [138]. Finally, Chen et al. [18] attempted to compare the reinforcing effect of pea starch nanocrystals and native pea granules in a PVA matrix. Even if the reinforcing effect of starch nanocrystals was clearly better than the one of the native granules, it remained very poor since only a very little improvement of strength and strain at break (10% at best) was noted for filler contents lower than 10 wt%. This was explained by the poor compatibility of both components [18].

Globally, waxy maize starch nanocrystals displayed a better reinforcing effect than pea starch nanocrystals, probably due to the higher size aspect ratio of waxy maize starch nanocrystals. Furthermore, the reinforcing effect of waxy maize starch nanocrystals is more significant in thermoplastic starch than in natural rubber due to stronger interactions between the filler and the amylopectin chains. The reinforcing effect of starch nanocrystals in thermoplastic starch may also be favoured by crystallization at the filler/matrix interface [134].

Table 6
Relative[a] rubbery storage tensile modulus (E'_R) and relative[a] tensile test characteristics (nominal Young modulus, E_R; nominal stress at break, σ_R; nominal strain at break, ε_R) for starch nanocrystals filled nanocomposites.

Matrix	Starch origin	RH (%)	Filler content (wt%)	E'_R	E_R	σ_R	ε_R	Year	Ref.
Poly(styrene-co-butyl acrylate)	Potato starch	0	5	2	–	–	–	1998	[139]
			10	4	–	–	–		
			20	22	–	–	–		
			30	100	–	–	–		
			40	400	–	–	–		
			60	1000	–	–	–		
Poly(styrene-co-butyl acrylate)	Waxy maize	0	10	2	–	–	–	2005	[114]
			30	5	–	–	–		
			50	100	–	–	–		
Natural rubber	Waxy maize	0	2	–	1.5	1.2	0.95	2005	[126]
			5	2	2.5	1.9	0.91		
			10	10	7.5	3.0	0.90		
			15	–	19.2	3.1	0.81		
			20	75	40.8	3.9	0.76		
			25	–	52.8	3.2	0.67		
			30	200	119.7	2.4	0.49		
Thermoplastic waxy maize starch/25 wt% of glycerol	Waxy maize	43	2	–	4.8	3.3	0.41	2006	[134]
			5	1.7	7.3	3.6	0.32		
			10	4.7	7.5	4.2	0.19		
			15	7.2	22	9.8	0.07		
Thermoplastic waxy maize starch/25 wt% of sorbitol	Waxy maize	43	5	1.5	2.1	2.6	0.90	2007	[132]
			10	2.0	2.2	3.8	0.92		
			15	2.5	2.7	4.2	0.65		
Pullulan/30 wt% of sorbitol	Waxy maize	53	3	2	2.3	1.5	0.58	2007	[136]
			6	–	2.5	1.7	0.50		
			15	9	7	2.6	0.27		
			20	–	8.6	2.9	0.21		
			40	–	15.5	5.1	0.06		
Waterbone polyurethane	Potato	–	1	1	1.1	2.4	1.4	2008	[17]
			2	0.93	1.1	2.5	1.7		
			4	0.2	1.1	3	1.4		
			5	0.2	1.9	4.7	1.2		
			8	1.1	1.7	3.4	1.1		
	Pea	0	5	–	2	2.5	0.87	2011	[130]
			10	–	37	2.7	0.75		
			20	–	65	2.2	0.63		
			30	–	67	1.1	0.36		
Poly(vinyl alcohol)	Pea	43	5	–	–	1.1	1.04	2008	[18]
			10	–	–	1.1	1.03		
			15	–	–	0.9	1		
			20	–	–	0.8	0.9		
			30	–	–	0.7	0.8		
			40	–	–	0.6	0.75		
Thermoplastic cassava starch/33 wt% of glycerol	Waxy maize	43	2.5	3.9	–	–	–	2009	[132]
Soy protein isolate/30 wt% glycerol	Pea	0	1		2.4	1.4	0.35	2009	[136]
			2		2.9	1.5	0.3		
			4	–	2.5	1.3	0.2		
			8		2.3	1.25	0.4		
			12	–	2	1	0.25		
			16		1.9	0.9	0.07		
Poly(butylene succinate)	Pea	0	5	–	1.02	1.03	1.2	2011	[138]
			10	–	1.12	0.85	1.1		
			15	–	1.15	0.55	0.6		
			20	–	1.2	0.46	0.3		
Carboxymethyl chitosan	Waxy maize	65	6	–	–	1.2	0.85	2011	[137]
			10	–	–	1.25	0.8		
			20	–	–	1.7	0.6		
			30	–	–	1.8	0.5		
			40	–	–	1.7	0.3		

[a] All properties are reported as the ratio between the properties of composites and the properties of the neat matrix. They are not absolute values.

6.2.2. Effect of surface modification/chemical grafting

The first attempt to chemically modify the surface of starch nanocrystals consisted in grafting small molecules using the hydroxyl groups from the nanoparticle surface to broaden the number of possible compatible polymeric matrices. Indeed, the chemical modification can be used for transforming the polar hydroxyl group sitting at the surface of starch nanocrystals in moieties capable of enhancing interactions with non-polar polymers. The two mechanisms chosen were esterification with the anhydride function of alkenyl succinic anhydride (ASA) and the formation of urethane using an isocyanate such as phenylisocyanate (PI) [71]. Modified starch nanocrystals were introduced in a NR matrix

using a casting/evaporation technique involving toluene as the liquid phase. Their reinforcing effect was compared to the one reported for unmodified nanoparticles filled systems [126]. DMA experiments demonstrated that the reinforcing effect of chemically modified starch nanocrystals in the rubbery state of the NR matrix was considerably reduced, as well as the thermal stability of the materials. Tensile tests confirmed that the reinforcing effect of starch nanocrystals displayed through the tensile modulus was much lower for modified nanocrystals than for unmodified ones. The ultimate properties (strength and strain at break) were also significantly affected. This was ascribed to the coating of SNC with the grafting agent, thus hindering the establishment of interactions through hydrogen bonds between chemically modified SNC [126]. Although modification by chemical reaction of small molecules on starch nanocrystals improved the adhesion between the filler and the matrix, it was demonstrated that it resulted in a sharp decrease in mechanical performance owing to the partial or total destruction of the three-dimensional network in the nanocomposites [126,127].

In this context, the strategy of "grafting onto" polymer chains was then applied to starch nanocrystals with various polymers such as poly(ethylene glycol) monobutyl ether (PEGME) [85], poly(propylene glycol) monobutyl ether (PPGBE), poly(tetrahydrofuran) (PTHF), polycaprolactone (PCL) [96] and styrene [98]. However, there are still shortcomings such as low controllability and grafting efficiency, as well as difficulty in grafting long-chain polymers [92]. To our knowledge, nanocomposite materials have not been yet prepared based on this method.

The "grafting from" strategy has been recently proposed. By this method, the polymerization of monomers and chain propagation of polymers are induced, and ultimately the polymer chains are coupled with the starch nanocrystals. In the study of Yu et al. [19], poly (ε-caprolactone) was grafted onto the surface of pea starch nanocrystals via microwave-assisted ring-opening polymerization based on "grafting from" strategy, and the resultant nanoparticles were used as filler in poly(lactic acid) (PLA) as matrix. Authors reported that the process of grafting PCL chains destroyed the starch nanocrystals aggregates and, hence, produced nano-objects with a relatively uniform size. It resulted in a simultaneous enhancement in strength (from about 42 to 58 MPa) and elongation at break (from about 10% to 135%) together with a decrease in Young modulus (from about 2000 to 1500 MPa) for a filler content of 5 wt%. However, when the loading was higher ($\geqslant$10 wt%) ultimate properties were dramatically decreased. This was attributed to the introduction of the PCL component, which provided flexibility to the nanocomposites, as well as the formation of an interfacial layer, which facilitated the stress transfer to rigid starch nanocrystals [19]. In continuation, PCL-grafted pea starch nanocrystals were incorporated into a waterbone polyurethane (WPU) matrix [109]. Authors also noted that the lowest loading level of 5 wt% resulted in a maximum tensile strength (from about 31 to 40 MPa), but contrarily to PLA, the elongation at break remained stable up to a filler content of 25 wt% while Young modulus increased strongly, with a maximum value for a filler content of 20 wt% (increase from about 1 up to 220 MPa for a filler content of 20 wt%) [109]. This enhancement was attributed to the uniform dispersion of grafted starch nanocrystals because of their nanoscale size, the increased entanglements mediated with grafted PCL chains, and the reinforcing function of rigid starch nanocrystals. With an increase of the filler content, the rubbery PCL component increased, inducing the self-aggregation of starch nanocrystals as crystalline domains, which impeded improvement in tensile strength and elongation at break, but significantly enhanced Young modulus [109].

In conclusion, the possibility of surface chemical modification of starch nanocrystals to improve the affinity between the filler and the polymer matrix opens large windows of applications. However, the effectiveness of interactions at the interfacial region between the reinforcements and the polymer matrix to enlarge the use and commercialization of biodegradable nanocomposites based on starch nanocrystals continues to be a challenge.

6.2.3. Reinforcing mechanisms

The reinforcing effect of starch nanocrystals is generally ascribed to the formation of a hydrogen bonded percolating filler network above a given starch content corresponding to the percolation threshold. This percolation phenomenon was evidenced in the case of natural rubber (NR) reinforced with waxy maize starch nanocrystals from swelling experiments (toluene and water uptake) for which changing behaviour was reported above a certain filler concentration [127]. In that case, the percolation threshold was estimated at 10 wt% [126]. The percolation mechanism has been verified by successive tensile experiments, which consisted in stretching the material to a given elongation, releasing the force, stretching again to a higher elongation, and repeating [127,140]. It was shown that for the unfilled NR matrix, the tensile modulus continuously increased during successive cycles due to the strain-induced crystallization of NR, whereas for highly filled nanocomposite materials the tensile modulus decreased during the five first cycles [127]. This was ascribed to the progressive disruption of the continuous starch nanocrystals network. The establishment of a percolating network was further confirmed by the same authors. They showed that any deterioration of these filler–filler interactions, for example induced by the surface chemical modification of starch nanocrystals, results in a dramatic decrease of the mechanical performances of the ensuing composites [126,127].

Recently, new highlights have been given concerning the reinforcing mechanisms of starch nanocrystals in NR matrix [129]. The presence of both Mullins and Payne effects was demonstrated, even for low filler contents, suggesting that the strain dependence of the viscoelastic properties of filler non-vulcanized NR could not be only related to the development of filler–filler interactions [129]. Two phenomenological models were used to predict the Payne effect and thus discriminate the possible origins of the non-linear viscoelastic behaviour: (i) the Kraus model considering that filler–filler interactions are preponderant and (ii) the Maier and Göritz model that is based on matrix-filler interactions. The use of the Kraus model provided the confirmation of the formation of a percolating network for filler contents higher than 6.7 vol% (10 wt%) [129]. However, the Kraus model was unable to predict the dissipative properties of the different nanocomposites. The use of the Maier and Goritz model allowed demonstrating that phenomena of adsorption and desorption of NR chains on the filler surface governed non-linear viscoelastic properties, even if the formation of a percolating network for filler contents >6.7 vol% (10 wt %) was evidenced [129]. The occurrence of interactions through the establishment of hydrogen bonds between the polymer matrix and starch nanocrystals was also clearly evidenced in the case of carboxymethyl chitosan [137] and WPU [130] based nanocomposites by FTIR analysis.

6.3. Water sensitivity and barrier properties

6.3.1. Water uptake

The water sensitivity of starch nanocrystals-based nanocomposites has been evaluated through the measurement of water uptake (WU), either in the form of vapour or liquid. It was measured for natural rubber [126], thermoplastic starch [132], pullulan [135], soy proteins [136] and carboxymethyl chitosan [137] based matrices.

In the case of natural rubber filled with waxy maize starch nanocrystals, liquid water uptake kinetics was carried out until

weight equilibrium (reached after 7 h of soaking) for filler contents up to 50 wt% [128]. It was shown that all the compositions absorbed liquid water during immersion, even the unfilled matrix. For the neat matrix and very low starch contents (up to 2 wt%), the liquid water uptake increased slightly during all the duration of the experiment. For starch contents higher than 2 wt%, the water uptake increased rapidly during the early stage of immersion, i.e., during the two or three first hours, and then decreased until reaching a plateau after 7 h of immersion. This diminution in the water uptake for long durations of immersion was attributed to the release of low molecular mass NR chains, but overall to the partial release, or leaching, of starch nanoparticles in water, even though starch is insoluble in water. This was particularly marked for filler contents higher than 10 wt%. Such a "starch nanocrystals release" phenomenon was explained by the formation of a soft and weak interface between the filler and the NR matrix during exposure to water, due to the swelling of starch domains. It was hypothesised that this phenomenon was magnified for highly filled materials due to the increasing probability of appearance of starch nanocrystals on the surface of the film in direct contact with the liquid medium. Regarding the water uptake at equilibrium, it was not significantly affected for filler contents up to 10 wt%, whereas it increased more or less linearly for filler contents higher than 10 wt% up to ca. 4.7-fold for the 50 wt% filled film (Table 7). For highly filled materials, it was deduced that the loss of unbonded starch nanoparticles was compensated by the swelling of the in bulk starch nanocrystals still bonded to the matrix. In parallel, it was shown that the addition of starch nanocrystals induced an increase in liquid water diffusivity. Interestingly, the evolution of the liquid water diffusivity was not linear as a function of filler content. The diffusivity first increased slightly up to a starch content of 10 wt%, and then increased more rapidly and roughly linearly. The formation of a continuous polar network of starch nanocrystals within the NR matrix was supposed to favour the swelling of the films by water. Furthermore, it was deduced that a filler content of 10 wt% was a critical value in the swelling behaviour of NR/starch nanocrystals materials. By analogy with materials reinforced with cellulose whiskers, it was assumed that the formation of a rigid network of starch nanocrystals was governed by a percolation mechanism. The critical volume fraction of starch nanocrystals at the percolation was difficult to determine due to the ill-defined geometry of the percolating species but was supposed to be around 6.7 vol% (i.e. 10 wt%) [120].

In the case of pullulan/waxy maize starch nanocrystals systems, a different behaviour than the one reported for natural rubber was observed. Moisture sorption isotherms showed that the water vapour uptake of nanocomposites was decreased with increasing filler content under similar water activity (aw) conditioning, with a more pronounced difference at high moisture conditions (aw > 0.75) [135]. A special interest was given by the authors to results obtained at high relative humidity. At 94%RH, while the differences in water uptake of films with 6–15 wt% starch nanocrystal content were small, appreciable less water was absorbed by samples filled with high amounts of SNC (20, 30 and 40 wt%) (Table 7). Such a reduction of the water sensitivity was also reported with carboxymethyl chitosan, which is also a water-soluble polymer [137]. In the case of reinforced carboxymethyl chitosan systems, the water uptake of films, which was evaluated at 93%RH, was first decreased dramatically by a factor of 2 with the increasing of the nanocrystal content up to 10 wt%, then decreased slightly with the increasing of the nanocrystals content to 30 wt% and finally remained constant for higher filler contents (Table 7). For these two water sensitive matrices, different mechanisms were proposed to explain the reduction of water sensitivity with increasing starch nanocrystals contents. The first proposed mechanism is based on a simple rule of mixture. Although starch nanocrystals are hydrophilic, such matrices may adsorb more water than starch crystallites, particularly at high water activities (aw > 0.8) [141]. Thus, the diminution of the proportion of the polymer matrix (considering the total dry matter of the sample) with the increment of starch nanocrystal content was ascribed to have, at least partially, a contribution to the decrease of water sensitivity of the composite films. The second proposed mechanism was that the reduction of the water sensitivity was also attributed to either the formation of a rigid three-dimensional starch nanocrystal network (due to the strong hydrogen bonding between the starch particles, as previously highlighted by Angellier et al. [126]) that prevents the swelling of the matrix. The last mechanism proposes that strong interactions between the filler and polymer chains decreases the swelling and water absorbance of the polymeric chains located in the interfacial regions [135,137].

Table 7
Relative water uptake (WU_R) of starch nanocrystals filled nanocomposites.

Matrix	Starch origin	Form of water	RH (%)	Filler content (wt%)	WU_R	Year	Ref.
Natural rubber	Waxy maize	Liquid	–	2	1.3	2005	[127]
				5	1.1		
				10	0.9		
				15	1.3		
				20	2		
				30	3.1		
				40	3.7		
				50	4.7		
Pullulan/30 wt% of sorbitol	Waxy maize	Vapour	94	3	0.97	2007	[135]
				10	0.92		
				15	0.89		
				20	0.81		
				30	0.76		
				40	0.72		
Cassava starch	Waxy maize	Vapour	98	2.5	1.43	2009	[132]
Carboxymethyl chitosan	Waxy maize	Vapour	93	3	0.82	2011	[137]
				6	0.69		
				10	0.52		
				20	0.42		
				30	0.32		
				40	0.32		

Such a reduction of the water sensitivity of hydrophilic matrices was not unanimous. For example in the case of soy proteins, the water sensitivity of materials was not significantly impacted by the incorporation of starch nanocrystals [129] while it was increased in the case of thermoplastic cassava starch reinforced with 2.5 wt% of waxy maize starch nanoparticles [132] (Table 7). In the case of the thermoplastic cassava starch systems, this effect was attributed to a better affinity of glycerol for starch nanocrystals than for the cassava starch matrix, leading to a cassava starch matrix with more OH-groups available to interact with moisture, as compared to the unfilled film. Furthermore, it is worth noting that for such low filler contents, there should not be no percolating network to reduce the swelling of the cassava starch matrix [132].

In conclusion, no general tendency could be drawn as regards the impact of starch nanocrystals on the water sensitivity of polymer matrices and should thus be studied case by case. The water sensitivity of starch nanocrystals based nanocomposites was first demonstrated to depend on the nature of the polymer and thus on the level of interactions between the filler and the matrix. In the case of apolar polymer matrices such as natural rubber, the water uptake was clearly increased by the introduction of nanocrystals while it was decreased, unchanged or only slightly increased in the case of hydrophilic matrices. Such a discrepancy could arise from the differences in compatibility between filler and matrix. The similar polar and hydrophilic character of matrix (biopolymers like starch or soy protein) and starch nanoparticles may lead to strong interactions between the filler and the matrix due to hydrogen bonding, which intensifies with increasing filler concentration, thus contributing to the evidenced lower water sensitivity of the highly hydrophilic composites such as pullulan [135] or carboxymethyl chitosan [137]. On the other hand, the inclusion of polar and hydrophilic particles within hydrophobic matrices, which easily and strongly bond with water, logically leads to an increase in water uptake of the composites compared with the unfilled hydrophobic matrix. Furthermore, the poor interfacial compatibility of such hydrophilic particles with hydrophobic polymeric matrixes (e.g. natural rubber) could result in a weak adhesion between filler and matrix and in low dispersion level of filler, thus favouring the adsorption of water.

The filler content as well as filler–filler interactions, which govern the formation of a starch nanocrystals percolating network, were also demonstrated to be important parameters governing the water sensitivity of starch nanocrystals based nanocomposites. For example in the case of hydrophilic matrices, it seems primordial to get a tight percolating network to achieve a significant reduction of the water uptake of materials. Finally, such water uptake experiments were revealed to be useful to get knowledge on the structure of materials, e.g. percolation threshold, as well as on the types and/or level of interactions between the different constituents of the system.

6.3.2. Water vapour and oxygen permeability

Barrier properties were evaluated in terms of water vapour and/or oxygen permeability. Globally, the incorporation of starch nanocrystals allowed to significantly reduce the water vapour and oxygen permeability of tested polymer matrices, i.e. natural rubber [126], pullulan [135], thermoplastic starch [132] and carboxymethyl chitosan [137]. This was ascribed to the formation of a tortuous diffusive pathway induced by the incorporation of platelet-like nanoparticles. It was shown that an increase in the starch nanocrystals content allowed to induce the formation of a percolating network, in favour of a more pronounced reduction of gas permeability [126,135]. However, it is worth noting that the level of permeability reduction as well as the optimal filler content were not the same depending on the tested matrices.

In the case of natural rubber, water vapour and oxygen decreased continuously upon starch nanocrystals addition together with the diffusivity [126] (Table 8). This reduction in permeability was all the more marked for nanocrystals content up to 10 wt%. In the case of a pullulan based matrix, a filler content higher than 20 wt% was required to get a significant reduction in water vapour diffusivity and thus in permeability [135] whereas the water vapour permeability of a cassava starch based matrix was decreased by 40% with only 2.5 wt% of starch nanocrystals (Table 8). In the case of carboxymethyl chitosan, the water vapour permeability of nanocomposites decreased radically with increasing nanocrystal content up to 20 wt% and then remained almost unchanged with increasing further the nanocrystal content (Table 8) [137]. Such a result was ascribed to the formation of aggregates above 30 wt% that may prevent the diffusion of water molecules [137].

An opposite result was obtained by Garcia et al. [133] for thermoplastic waxy maize starch/waxy maize starch nanocrystals systems for which an increase in water vapour permeability was noticed (Table 8). This unexpected result was explained by the closed interactions of starch nanocrystals with glycerol, thus forming threads with high concentration of OH and thus, forming a preferential path for water vapour diffusion through the nanothreads [133].

Table 8
Relative water vapour permeability (WVP_R) of starch nanocrystals filled nanocomposites.

Matrix	Starch origin	Conditions	Filler content (wt%)	WVP_R	Year	Ref.
Natural rubber	Waxy maize	Between 0 and 50%RH	10	0.71	2005	[127]
			20	0.55		
			30	0.35		
Pullulan/30 wt% of sorbitol	Waxy maize	Between 53 and 100%RH	3	1.03	2007	[135]
			10	1.04		
			15	1.07		
			20	1.05		
			30	0.80		
			40	0.78		
Cassava starch	Waxy maize	Between 0 and 58%RH	2.5	0.6	2009	[132]
Carboxymethyl chitosan	Waxy maize	Between 0 and 83%RH	3	0.83	2011	[137]
			6	0.75		
			10	0.58		
			20	0.23		
			30	0.25		
			40	0.25		
Waxy maize starch	Waxy maize	Between 0 and 58%RH	2.5	1.78	2011	[134]

7. Conclusions and perspectives

The increasing scientific and industrial interest for starch nanoparticles (SNP) has led to the development of numerous methods for preparing sub-micron starch fillers for nanocomposites applications. Starch nanocrystals (SNC) are one type of SNP with crystalline property and platelet like morphology which depend on the nature of the native starch. SNC have been extracted from various botanical sources including normal maize, waxy maize, amylomaize, potato, rice, oat, peas or beans. Ensuing SNC have various amylose content, shape, viscosity in suspension, surface reactivity and thermal resistance. To date, the most common method for extracting SNC remains the mild hydrolysis of the amorphous parts of native granular starch. So far, alternative methods render much lower yield.

Since the first publications on SNC, the principal aim is to use them as reinforcement in polymer matrices. The reinforcing effect and mechanism in various poly(styrene-co-butyl acrylate) [114,139], natural rubber [125–129], starch [131–134], pullulan [135], soy proteins [136], or carboxymethyl chitosan [137], has been largely reported to have a positive effect. Thanks to the reactive nature of starch, SNC can be modified by grafting or cross-linking which renders them more readily dispersible in the polymer matrix. Due to its relatively high crystallinity and platelet shape, SNC have also been considered for barrier property (water vapour, oxygen) applications.

As the number of journal articles on the use of SNC continues to grow, there is a need to further optimize the production process. First, although the yield of extraction of SNC by batch might be optimum [50], further work should focus on continuous processes such as described by LeCorre et al. [114]. Second, another limitation in the use of SNC sits in its extraction as an aqueous suspension. The production of redispersible SNC – as it has been done with cellulose nanocrystals and nanofibres [115] – would be highly desirable. It would enable better control over the amount of SNC used for reinforcement, and increase the number of polymers to be used as matrix.

References

[1] Pliny the Elder, Book XIII, in: Pliny (Ed.), The Natural History, AD 77–79 (Chapter 17 and 26).
[2] A. Revedin, B. Aranguren, R. Becattini, L. Longo, E. Marconi, M.M. Lippi, N. Skakun, A. Sinitsyn, E. Spiridonova, J. Svobodahi, Proc. Natl. Acad. Sci. USA 107 (2010) 18815–18819.
[3] Association des Amidonniers et Féculiers, 2009.
[4] K.C. Huber, J.N. BeMiller, Modified starch: chemistry and properties, in: A.C. Bertolini (Ed.), Starches: Characterization, Properties and Applications, CRC Press, Boca Raton, 2010, pp. 145–203.
[5] R.L. Whistler, J. BeMiller, Starch: Chemistry and Technology, third ed., Elsevier, New York, 2009.
[6] J.R. Daniel, R.L. Whistler, H. Röper, Starch, in: Wiley (Ed.), Ullmann's Encyclopedia of Industrial Chemistry 2007, VCH Verlag GmbH & Co, 2000.
[7] D.J. Gallant, B. Bouchet, P.M. Baldwin, Carbohydr. Polym. 32 (1997) 177–191.
[8] A. Dufresne, Polymer nanocomposites from biological sources, in: A.C. Bertolini (Ed.), Biopolymers Technology, Sao Paulo, Brazil, 2007, pp. 59–83.
[9] C.G. Oates, Trends Food Sci. Technol. 8 (1997) 375–382.
[10] J.M.V. Blanshard, Starch granule structure and function: a physicochemical approach, in: T. Galliard (Ed.), Starch: Properties and Potentials, Society of Chemical Industry, London, UK, 1987, pp. 16–54.
[11] J.-L. Jane, J.J. Shen, Carbohydr. Res. 247 (1993) 279–290.
[12] T. Kasemsuwan, J. Jane, Cereal Chem. 71 (1994) 282–287.
[13] S. Pérez, P. Baldwin, D.J. Gallant, Structural features of starch granules I, in: R. L. Whistler, J. BeMiller (Eds.), Starch: Chemistry and Technology, Elsevier, New York, 2009.
[14] J.C. Shannon, D.L. Garwood, C.D. Boyer, Genetic and physiology of starch development, in: J. BeMiller, R. Whistler (Eds.), Starch: Chemistry and Technology, third ed., Academic Press, Elsevier, 2009, p. 28.
[15] D. Le Corre, J. Bras, A. Dufresne, Biomacromolecules 11 (2010) 1139–1153.
[16] J.L. Putaux, S. Molina-Boisseau, T. Momaur, A. Dufresne, Biomacromolecules 4 (2003) 1198–1202.
[17] G. Chen, M. Wei, J. Chen, J. Huang, A. Dufresne, P.R. Chang, Polymer 49 (2008) 1860–1870.
[18] Y. Chen, X. Cao, P.R. Chang, M.A. Huneault, Carbohydr. Polym. 73 (2008) 8–17.
[19] J. Yu, F. Ai, A. Dufresne, S. Gao, J. Huang, P.R. Chang, Macromol. Mater. Eng. 293 (2008) 763–770.
[20] H. Zheng, F. Ai, P.R. Chang, J. Huang, A. Dufresne, Polym. Compos. 30 (2009) 474–480.
[21] N.L. Garcia, L. Ribba, A. Dufresne, M.I. Aranguren, S. Goyanes, Macromol. Mater. Eng. 294 (2009) 169–177.
[22] H. Namazi, A. Dadkhah, Carbohydr. Polym. 79 (2010) 731–737.
[23] Y. Wang, L. Zhang, J. Nanosci. Nanotechnol. 8 (2008) 5831–5838.
[24] 王才, 潘则林, 赵萍, 吴美琰, Google Patents, 2013.
[25] J. Huang, G. Chen, A. Dufresne, M. Wei, G. Cui, 20070822, 2007.
[26] J. Huang, F. Yi, R. Zhang, W. Xia, M. Wei, 20080730, 2008.
[27] 任丽丽, 佟金, 周江, 孙霁宇, 蒋蔓, 陈东辉, 马云海, Google Patents, 2012.
[28] 金征宇, 田耀旗, 魏本喜, 陈煌莉, 胡秀婷, 徐学明, 谢正军, 赵建伟, Google Patents, 2013.
[29] 黄进, 艾福金, 魏铭, 郑化, Google Patents, 2007.
[30] S.N. Goyanes, M.I. Aranguren, N.L. García, L.M. Fama, L. Ribba, A. Dufresne, Google Patents, 2011.
[31] 孙庆杰, 熊柳, 李广华, Google Patents, 2013.
[32] 金征宇, 田耀旗, 魏本喜, 胡秀婷, 陈煌莉, 赵建伟, 徐学明, 谢正军, Google Patents, 2013.
[33] X. Ma, R. Jian, P.R. Chang, J. Yu, Biomacromolecules 9 (2008) 3314–3320.
[34] Y. Tan, K. Xu, L. Li, C. Liu, C. Song, P. Wang, ACS Appl. Mater. Interfaces 1 (2009) 956–959.
[35] J.-Y. Kim, S.-T. Lim, Carbohydr. Polym 76 (2009) 110–116.
[36] D. Liu, Q. Wu, H. Chen, P.R. Chang, J. Colloid Interface Sci. 339 (2009) 117–124.
[37] A.C.F. Ip, T.H. Tsai, I. Khimji, P.-J.J. Huang, J. Liu, Carbohydr. Polym. 110 (2014) 354–359.
[38] A. Hebeish, M.H. El-Rafie, M.A. El-Sheikh, M. El-Naggar, J. Inorg. Organomet. Polym Mater. 24 (2014) 515–524.
[39] S.T. Lim, J.Y. Kim, 2008. CAPLUS AN 2008:1490656 (Patent).
[40] S.T. Lim, J.Y. Kim, 2009. CAPLUS AN 2009:679477 (Patent).
[41] J.-Y. Kim, D.-J. Park, S.-T. Lim, Cereal Chem. 85 (2008) 182–187.
[42] Ecosynthetix, Ecosphere brochure, 2010. Available from: <http://www.ecosynthetix.com/ecosphere.html>.
[43] F.E. Giezen, R.O.J. Jongboom, H. Feil, K.F. Gotlieb, A. Boersma, 2000. CAPLUS AN 2000:824306 (Patent).
[44] C. Bastioli, G. Floridi, G.D. Tredici, 2008. WO2008037749 (A2) (Patent).
[45] C. Bastioli, G. Floridi, G.D. Tredici, 2009. US 2009/03114455 (A1) (Patent).
[46] Novamont, MaterBi Company Brochure, 2009. Available from: <http://www.materbi.com/ing/html/PDF/company_brochure.pdf>.
[47] B. Ma, X. Zhu, 2009. CAPLUS AN 2009:1548291 (Patent).
[48] X. Liu, S. Xiao, B. Liu, J. Liu, D. Tang, 2003. CAPLUS AN 2005:148270 (Patent).
[49] A. Dufresne, J.Y. Cavaille, W. Helbert, Macromolecules 29 (1996) 7624–7626.
[50] H. Angellier, L. Choisnard, S. Molina-Boisseau, P. Ozil, A. Dufresne, Biomacromolecules 5 (2004) 1545–1551.
[51] L. Jayakody, R. Hoover, Food Res. Int. 35 (2002) 665–680.
[52] C.G. Biliaderis, D.R. Grant, J.R. Vose, Cereal Chem. 58 (1981) 496–502.
[53] D. French, Organization of starch granules, in: R.L. Whistler, J.N. BeMiller, E.F. Paschall (Eds.), Starch: Chemistry and Technology, New York, USA, Academic Press, 1984, pp. 183–247.
[54] B. Wei, X. Hu, B. Zhang, H. Li, X. Xu, Z. Jin, Y. Tian, Int. J. Biol. Macromol. 62 (2013) 652–656.
[55] V. Singh, S.Z. Ali, Starch – Stärke 39 (1987) 402–405.
[56] V. Singh, S.Z. Ali, Starch – Staerke 45 (1993) 59–62.
[57] V. Singh, S.Z. Ali, Carbohydr. Polym. 41 (2000) 191–195.
[58] V. Singh, S.Z. Ali, Int. J. Food Prop. 11 (2008) 495–507.
[59] D. Le Corre, J. Bras, L. Choisnard, A. Dufresne, Starch – Stärke 64 (2012) 489–496.
[60] H. Angellier, Material Sciences, University Joseph Fourier, Grenoble, France, 2005. p. 285.
[61] B. Wei, X. Xu, Z. Jin, Y. Tian, PLoS One 9 (2014) e86024.
[62] M. Nitschke, A.C. Bertolini, M.A.V. Teixeira, C.F. Garcia, Biopolymers on food technology: production and applications of modified starches, in: A.C.E. Bertolini (Ed.), Biopolymers Technology, Cultura Acadêmica, São Paulo, 2007, p. 199. pp. 113–144.
[63] H. Angellier-Coussy, J.-L. Putaux, S. Molina-Boisseau, A. Dufresne, E. Bertoft, S. Perez, Carbohydr. Res. 344 (2009) 1558–1566.
[64] H.-Y. Kim, J.-A. Han, D.-K. Kweon, J.-D. Park, S.-T. Lim, Carbohydr. Polym. 93 (2013) 582–588.
[65] M.L. Foresti, M.d.P. Williams, R. Martínez-García, A. Vázquez, Carbohydr. Polym. 102 (2014) 80–87.
[66] D. LeCorre, E. Vahanian, A. Dufresne, J. Bras, Biomacromolecules 13 (2012) 132–137.
[67] S. Bel Haaj, A. Magnin, C. Pétrier, S. Boufi, Carbohydr. Polym. 92 (2013) 1625–1632.
[68] J. Zhu, L. Li, L. Chen, X. Li, Food Hydrocolloids 29 (2012) 116–122.
[69] H.-Y. Kim, D.J. Park, J.-Y. Kim, S.-T. Lim, Carbohydr. Polym. 98 (2013) 295–301.
[70] Q. Sun, G. Li, L. Dai, N. Ji, L. Xiong, Food Chem. 162 (2014) 223–228.
[71] R.L. Whistler, J.N. BeMiller, E.F. Paschall, Starch: Chemistry and Technology, second ed., New York and London, 1967.
[72] A. Imberty, S. Perez, Biopolymers 27 (1988) 1205–1221.
[73] A. Imberty, H. Chanzy, S. Perez, A. Buleon, V. Tran, Macromolecules 20 (1987) 2634–2636.
[74] A. Luc, J.H. Peter, Biofuels, Bioprod. Biorefin. 3 (2009) 329–343.
[75] D. LeCorre, J. Bras, A. Dufresne, J. Nanopart. Res. 13 (2011) 7193.

[76] J.-P. Robin, Institut National de la Recherche Agronomique (INRA), Université Pierre et Marie Curie de Paris, Nancy, 1976.
[77] S.J. McGrance, H.J. Cornell, C.J. Rix, Starch – Stärke 50 (1998) 158–163.
[78] J. Araki, M. Wada, S. Kuga, T. Okano, J. Wood Sci. 45 (1999) 258–261.
[79] H. Angellier, S. Molina-Boisseau, M.N. Belgacem, A. Dufresne, Langmuir 21 (2005) 2425–2433.
[80] C. Li, P. Sun, C. Yang, Starch – Stärke 64 (2012) 497–502.
[81] D. Cooke, M.J. Gidley, Carbohydr. Res. 227 (1992) 103–112.
[82] Z. Zhong, X.S. Sun, J. Food Eng. 69 (2005) 453–459.
[83] S.a.L. Randzio, I. Flis-Kabulska, J.-P.E. Grolier, Macromolecules 35 (2002) 8852–8859.
[84] P. Colonna, A. Buleon, Thermal transitions of starches, in: A.C. Bertolini (Ed.), Starches: Characterization, Properties, and Applications, CRC Press, NW, 2010, pp. 71–102.
[85] N. Atichokudomchai, S. Varavinit, P. Chinachoti, Starch – Stärke 54 (2002) 296–302.
[86] T.A. Waigh, M.J. Gidley, B.U. Komanshek, A.M. Donald, Carbohydr. Res. 328 (2000) 165–176.
[87] C.G. Biliaderis, C.M. Page, T.J. Maurice, B.O. Juliano, J. Agric. Food Chem. 34 (1986) 6–14.
[88] J.W. Donovan, Biopolymers 18 (1979) 263–275.
[89] I.D. Evans, D.R. Haisman, Stärke 34 (1982).
[90] C.G. Biliaderis, C.M. Page, L. Slade, R.R. Sirett, Carbohydr. Polym. 5 (1985) 367–389.
[91] C. Barron, ISITEM, Université de Nantes, Nantes, 1999. p. 164.
[92] T.A. Waigh, K.L. Kato, A.M. Donald, M.J. Gidley, C.J. Clarke, C. Riekel, Starch – Stärke 52 (2000) 450–460.
[93] W. Thielemans, M.N. Belgacem, A. Dufresne, Langmuir 22 (2006) 4804–4810.
[94] D. LeCorre, J. Bras, A. Dufresne, Carbohydr. Polym. 87 (2012) 658–666.
[95] K. Kümmerer, J. Menz, T. Schubert, W. Thielemans, Chemosphere 82 (2011) 1387–1392.
[96] Y. Habibi, A. Dufresne, Biomacromolecules 9 (2008) 1974–1980.
[97] G. Siqueira, J. Bras, A. Dufresne, Langmuir 26 (2010) 402–411.
[98] A. Junior De Menezes, G. Siqueira, A.A.S. Curvelo, A. Dufresne, Polymer 50 (2009) 4552–4563.
[99] A. Dufresne, Molecules 15 (2010) 4111–4128.
[100] N. Lin, J. Huang, P.R. Chang, D.P. Anderson, J. Yu, J. Nanomater. 2011 (2011) 13.
[101] N. Lin, J. Huang, A. Dufresne, Nanoscale 4 (2012) 3274–3294.
[102] N. Lin, J. Huang, P.R. Chang, L. Feng, J. Yu, Colloids Surf. B: Biointerfaces 85 (2) (2011) 270–279.
[103] Y. Xu, W. Ding, J. Liu, Y. Li, J.F. Kennedy, Q. Gu, S. Shao, Carbohydr. Polym. 80 (2010) 1078–1084.
[104] M. Labet, W. Thielemans, A. Dufresne, Biomacromolecules 8 (2007) 2916–2927.
[105] C. Wang, Z. Pan, M. Wu, P. Zhao, J. Appl. Polym. Sci. (2014).
[106] S. Song, C. Wang, Z. Pan, X. Wang, J. Appl. Polym. Sci. 107 (2008) 418–422.
[107] H. Namazi, A. Dadkhah, J. Appl. Polym. Sci. 110 (2008) 2405–2412.
[108] A.-L. Goffin, Science, Mons University, Mons, Belgium, 2010. p. 178.
[109] P.R. Chang, F. Ai, Y. Chen, A. Dufresne, J. Huang, J. Appl. Polym. Sci. 111 (2009) 619–627.
[110] L. Ren, M. Jiang, L. Wang, J. Zhou, J. Tong, Carbohydr. Polym. 87 (2012) 1874–1876.
[111] M.J. Jivan, A. Madadlou, M. Yarmand, Food Chem. 141 (2013) 1661–1666.
[112] L. Ren, M. Jiang, J. Zhou, J. Tong, Carbohydr. Polym. 87 (2012) 1874–1876.
[113] J. Yang, Y. Huang, C. Gao, M. Liu, X. Zhang, Colloids Surf. B: Biointerfaces 115 (2014) 368–376.
[114] D. LeCorre, J. Bras, A. Dufresne, Carbohydr. Polym. 86 (2011) 1565–1572.
[115] K. Missoum, J. Bras, M.N. Belgacem, Biomacromolecules 13 (2012) 4118–4125.
[116] A. Donald, P. Jenkins, T. Waigh, Council for the Central Laboratory of the Research Councils, 1997, p. 54.
[117] H. Tang, T. Mitsunaga, Y. Kawamura, Carbohydr. Polym. 63 (2006) 555–560.
[118] A.-M. Shi, D. Li, L.-J. Wang, B.-Z. Li, B. Adhikari, Carbohydr. Polym. 83 (2011) 1604–1610.
[119] A.-M. Shi, D. Li, L.-J. Wang, Y.-G. Zhou, B. Adhikari, J. Food Eng. 113 (2012) 399–407.
[120] D. Song, Y.S. Thio, Y. Deng, Carbohydr. Polym. 85 (2011) 208–214.
[121] W. Li, H. Corke, T. Beta, Carbohydr. Polym. 69 (2007) 398–405.
[122] H. Angellier, J.-L. Putaux, S. Molina-Boisseau, D. Dupeyre, A. Dufresne, Macromol. Symp. 221 (2005) 95–104.
[123] J.P. Robin, C. Mercier, R. Charbonniere, A. Guilbot, Cereal Chem. 51 (1974) 389–406.
[124] C. Hernández-Jaimes, L.A. Bello-Pérez, E.J. Vernon-Carter, J. Alvarez-Ramirez, Carbohydr. Polym. 95 (2013) 207–213.
[125] T.A. Waigh, P. Perry, C. Riekel, M.J. Gidley, A.M. Donald, Macromolecules 31 (1998) 7980–7984.
[126] H. Angellier, S. Molina-Boisseau, A. Dufresne, Macromolecules 38 (2005) 9161–9170.
[127] H. Angellier, S. Molina-Boisseau, L. Lebrun, A. Dufresne, Macromolecules 38 (9) (2005) 3783–3792.
[128] H. Angellier, S. Molina-Boisseau, A. Dufresne, Macromol. Symp. 233 (2006) 132–136.
[129] P. Mélé, H. Angellier-Coussy, S. Molina-Boisseau, A. Dufresne, Biomacromolecules 12 (2011) 1487–1493.
[130] J. Zou, F. Zhang, J. Huang, P.R. Chang, Z. Su, J. Yu, Carbohydr. Polym. 85 (2011) 824–831.
[131] J. Viguié, S. Molina-Boisseau, A. Dufresne, Macromol. Biosci. 7 (2007) 1206–1216.
[132] N.L. Garcia, L. Ribba, A. Dufresne, M. Aranguren, S. Goyanes, Macromol. Mater. Eng. 294 (2009) 169–177.
[133] N.L. Garcia, L. Ribba, A. Dufresne, M. Aranguren, S. Goyanes, Carbohydr. Polym. 84 (2011) 203–210.
[134] H. Angellier, S. Molina-Boisseau, P. Dole, A. Dufresne, Biomacromolecules 7 (2006) (2006) 531–539.
[135] E. Kristo, C.G. Biliaderis, Carbohydr. Polym. 68 (2007) 146–158.
[136] H. Zheng, F. Ai, P.R. Chang, J. Huang, A. Dufresne, Polym. Compos. 30 (4) (2009) 474–480.
[137] B. Duan, P. Sun, X. Wang, C. Yang, Starch – Stärke 63 (2011) 528–535.
[138] N. Lin, J. Yu, P.R. Chang, J. Li, J. Huang, Polym. Compos. 32 (3) (2011) 472–482.
[139] A. Dufresne, J.Y. Cavaillé, J. Polym. Sci. Part B: Polym. Phys. 36 (1998) 2211–2224.
[140] A. Dufresne, Can. J. Chem. 86 (6) (2008) 484–494.
[141] H. Bizot, P. Le Bail, B. Leroux, P. Roger, A. Buleon, Carbohydr. Polym. 40 (1997) 33–50.